Eur. Phys. J. C (2016) 76:50
DOI 10.1140/epjc/s10052-016-3896-0

THE EUROPEAN PHYSICAL JOURNAL C

Regular Article - Experimental Physics

Interpreting single jet measurements in Pb+Pb collisions at the LHC

Martin Spousta[1,a], **Brian Cole**[2,b]

[1] Institute of Particle and Nuclear Physics, Charles University, Prague, Czech Republic
[2] Physics Department and Nevis Laboratories, Columbia University, New York, NY 10027, USA

Received: 11 June 2015 / Accepted: 14 January 2016 / Published online: 27 January 2016

Abstract Results are presented from a phenomenological analysis of recent measurements of jet suppression and modifications of jet fragmentation functions in Pb+Pb collisions at the LHC. Particular emphasis is placed on the impact of the differences between quark and gluon jet quenching on the transverse momentum ($p_{\mathrm{T}}^{\mathrm{jet}}$) dependence of the jet R_{AA} and on the fragmentation functions, $D(z)$. Primordial quark and gluon parton distributions were obtained from PYTHIA8 and were parameterized using simple power-law functions and extensions to the power-law function which were found to better describe the PYTHIA8 parton spectra. A simple model for the quark energy loss based on the shift formalism is used to model R_{AA} and $D(z)$ using both analytic results and using direct Monte-Carlo sampling of the PYTHIA parton spectra. The model is capable of describing the full $p_{\mathrm{T}}^{\mathrm{jet}}$, rapidity, and centrality dependence of the measured jet R_{AA} using three effective parameters. A key result from the analysis is that the $D(z)$ modifications observed in the data, excluding the enhancement at low-z, may result primarily from the different quenching of the quarks and gluons. The model is also capable of reproducing the charged hadron R_{AA} at high transverse momentum. Predictions are made for the jet R_{AA} at large rapidities where it has not yet been measured and for the rapidity dependence of $D(z)$.

1 Introduction

Measurements of jet production and jet properties in ultra-relativistic nuclear collisions provide an important tool to study the properties of quark gluon plasma created in the collisions. High-energy quarks and gluons produced in hard-scattering processes can interact with and lose energy while propagating in the plasma. Those interactions can both reduce the energy of the jets that result from the fragmentation of the quarks and gluons and change the properties of the jets. These and other "medium" modifications of the parton showers initiated by the hard scattering [1,2] are frequently collectively referred to as "jet quenching".

Jet quenching was first observed at the LHC through the observation of highly asymmetric dijet pairs [3] that result when the two jets lose different amounts of energy in plasma. Since dijet pairs for which both jets lose similar energy or, more generally, have similar modifications will appear "symmetric", other observables are needed to probe the effects of quenching on the typical jet. Measurements of the suppression of the hadron spectrum resulting from the energy loss of the parent jets have been carried out at both RHIC [4–6] and the LHC [7–9]. These show a suppression that at the LHC varies from a factor ∼5 for hadron transverse momentum (p_{T}) values ∼10 GeV to a factor of ∼2 for $p_{\mathrm{T}} \gtrsim 50$ GeV. Most jet quenching calculations that attempt to infer medium properties such as the quenching transport parameter, $\hat{q}$ (see e.g. [10] and references therein) have relied on the single hadron suppression results because of the theoretical simplicity in calculating single hadron spectra. However, the single hadron measurements have only indirect sensitivity to the kinematics of the parent parton and little sensitivity to the details of the modification of the parton shower.

Recent measurements of the suppression of the jet yield in 2.76 TeV Pb+Pb collisions at the LHC [11] are expected to provide a more sensitive probe of the physics of jet quenching at least through the improved correlation between the measured jet and the parent parton (shower) kinematics. Recent measurements of the jet nuclear modification factor, R_{AA}, for high transverse momentum jets show a factor of ∼2 suppression in the jet yield that increases slowly with increasing $p_{\mathrm{T}}^{\mathrm{jet}}$. The suppression is observed to vary monotonically as a function of collision centrality and to be independent of jet rapidity within the statistical and systematic uncer-

[a] e-mail: martin.spousta@cern.ch
[b] e-mail: cole@nevis.columbia.edu

tainties. Separately, recent measurements of the fragmentation functions for jets produced in Pb+Pb collisions [12,13] have shown an enhanced yield of hadrons with low transverse momenta, p_{T}, or low jet momentum fraction, z, a suppressed yield of hadrons with $0.05 \lesssim z \lesssim 0.2$ and possibly an enhanced yield of hadrons with $z \gtrsim 0.2$. These two observables, the single jet suppression and the modification of the fragmentation function, arguably provide the minimal set of data needed to understand the physics of jet quenching: the jet suppression is sensitive to the amount of energy the jet loses – outside the jet "cone" – while the fragmentation function is sensitive to the re-distribution of energy inside the jet cone.

Interpretation of the inclusive jet suppression and fragmentation data is complicated by the flavor admixture of the primordial partons. For this analysis, we focus on the relative combination of light quarks and gluons which are expected to suffer different energy loss due to their different color charges and/or differences between the quark and gluon splitting functions. In weak coupling calculations, the relative quark and gluon energy loss rates are determined by perturbative QCD color factors. For example, it is usually assumed that gluons lose energy at a rate $9/4$ higher than that for quarks. Recent studies including those based on quenching Monte Carlo codes have been compared to the jet R_{AA} and fragmentation function measurements, but these analyses have not explicitly attempted to elucidate the role of the relative quark and gluon contributions to the jet spectrum.

In this paper, we attempt to interpret recent measurements of the single jet suppression and fragmentation function ratios explicitly accounting for the role of the quark and gluon admixture. We argue that some of the features of the data can be explained purely on the basis of the $p_{\mathrm{T}}^{\mathrm{jet}}$ dependence of the quark to gluon fraction of the primordial parton spectrum and the different quark and gluon energy loss. Our analysis is based on simple assumptions regarding the parametric dependence of the energy loss on the jet transverse momentum and flavor. These assumptions are sufficiently simple that the results of our analysis can be easily explained and understood, but their simplicity also means that the results presented here should be verified using a proper jet quenching calculation. Our analysis is based on a combination of analytic calculation and Monte Carlo simulation using simulated quark and gluon spectra obtained from PYTHIA8 [14].

The outline of the paper is as follows. First, the attempt to interpret the measured jet R_{AA} within a simple fractional energy loss model is described. In that model the energy lost by a jet depends linearly on $p_{\mathrm{T}}$of primordial parton and an effective color factor, c_F which captures differences in the quenching between the jets initiated by quarks and gluons. It is demonstrated that this model fails to describe the data on jet R_{AA}. Then, a model of non-constant fractional energy loss is explored. In that model the energy lost by a jet is proportional to an undetermined power of primordial parton p_{T} and quenching of quark and gluon initiated jets differs by the c_F. It is shown that this model can describe the centrality and rapidity dependence of the jet R_{AA} and the values of parameters are extracted for the choice of $c_F = 9/4$. It is also shown that the model is capable of describing some features seen in the fragmentation functions, namely: the enhancement of yields of hadrons with high-z, the suppression of yields of hadrons with low-z, and the high-p_{T} behavior of charged particle R_{AA}. Finally, predictions for the behavior of the jet R_{AA} and fragmentation functions is provided.

There are two key assumptions in the modeling presented in this paper: the parton shower loses the energy to the medium in a manner such that the lost energy does not appear within the jet "cone"; the fragmentation of the resulting jet is assumed to be the same as in vacuum. The first assumption is consistent with observations by CMS [15] indicating that the medium induced radiation flows to large angles. The second assumption is qualitatively consistent with studies of color-coherence effects [16,17] leading to the picture in which the internal structure of a jet is not resolved by the medium. Validity of these assumptions is further discussed in the discussion section of this paper. It should be clearly stated that the model in this paper is not meant to provide a full description of the physics of the jet quenching. The main aim of the modeling in this paper is to point to a possible common origin of various distinct features seen in the data. The model is lacking implementation of the fluctuating nature of energy loss as well as its path-length dependence. This means that the model only approximately parametrizes the convolution of the energy loss with the primordial jet spectrum and the parameters extracted from the model should be viewed as effective parameters. Such an approach to the modeling of some aspects of the jet quenching was used in past and it was demonstrated that it may be useful in probing the relevance of different physics mechanisms that are assumed to lead to the jet quenching [18–20].

2 Parameterizing jet spectra and $D(z)$ distributions

A key ingredient of the analysis in this paper is the quark and gluon jet spectra which were obtained from PYTHIA8 using procedures chosen to be similar to those used in certain ATLAS simulations [21,22]. Namely, PYTHIA8 was run using parameters from the AU2 tune [23] and using CT10 parton distribution functions [24]. This combination was shown to describe well the LHC jet data [22]. Jets were reconstructed using the anti-k_t algorithm [25] with the distance parameter $R = 0.4$ applied to hadrons with lifetimes $c\tau > 1$ mm. The resulting jets were matched to one of the two outgo-

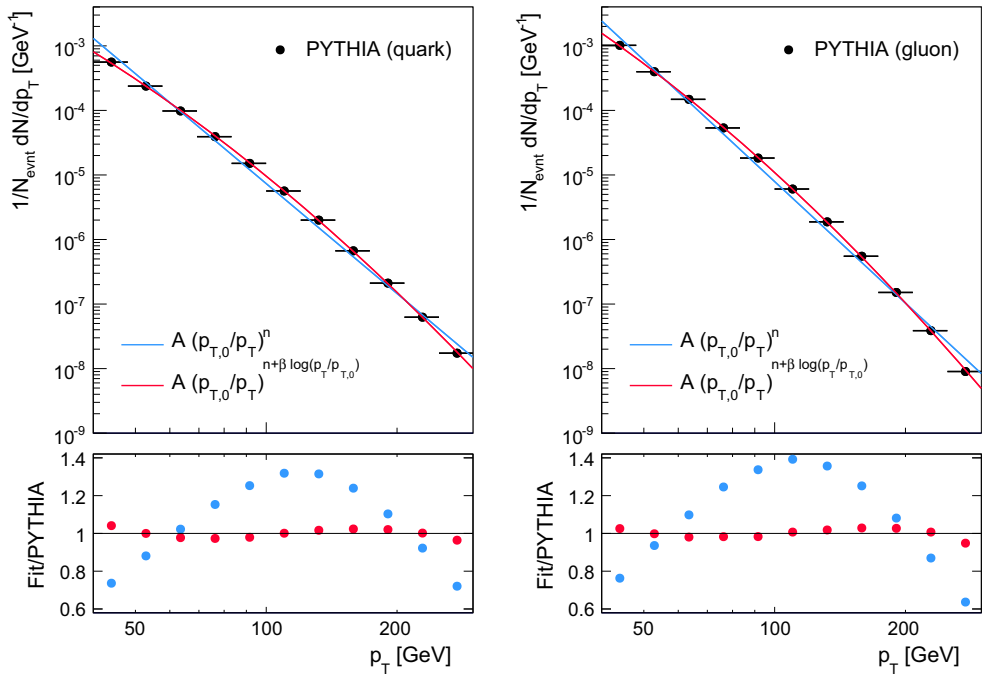

Fig. 1 *Top panels* quark (*left*) and gluon (*right*) spectra obtained from PYTHIA8 simulations over the rapidity interval $|y| < 2.1$ with simple power law (Eq. 1) and modified power law (Eq. 2) fits superimposed. *Bottom panels* ratios of the spectra to the two fit functions

Table 1 Parameters obtained from fits of the PYTHIA8 jet spectra to power-law (Eq. 1) and extended power-law (Eq. 2) functions

Fit type	Parameter	$\|y\| < 2.1$	$\|y\| < 0.3$	$0.3 < \|y\| < 0.8$	$1.2 < \|y\| < 2.1$
All	f_{q0}	0.34	0.28	0.29	0.40
Power law	n_q	5.66	5.37	5.40	6.15
	n_g	6.25	5.97	6.09	6.92
Extended power law	n_q	4.19	4.34	4.27	3.75
	β_q	0.71	0.49	0.54	1.2
	n_g	4.69	4.55	4.57	4.60
	β_g	0.80	0.71	0.76	1.2

ing partons from the leading order hard-scattering process by choosing the parton with the smallest angular distance, $\Delta R = \sqrt{\Delta\phi^2 + \Delta\eta^2}$ and the flavor of the jet was assigned to be that of the matched parton. Six million PYTHIA hard-scattering events were generated for each of five intervals of $\hat{p}_{\mathrm{T}}$, the transverse momentum of outgoing partons in the $2 \to 2$ hard-scattering, with boundaries 17, 35, 70, 140, 280 and 560 GeV.

The Monte Carlo results presented in this paper were obtained by directly using the jets obtained from the PYTHIA8 simulations, but the analytic results require a parameterization of the $p_{\mathrm{T}}^{\mathrm{jet}}$ dependence of the jet yields. A common parameterization used to describe the spectra of high-p_{T} hadrons or jets is the power-law form, e.g.

$$\frac{dn}{dp_{\mathrm{T}}^{\mathrm{jet}}} = A\left(\frac{p_{\mathrm{T0}}}{p_{\mathrm{T}}^{\mathrm{jet}}}\right)^{n}, \tag{1}$$

where p_{T0} is a reference transverse momentum value at which A represents $dn/dp_{\mathrm{T}}^{\mathrm{jet}}$. Results of fits to the quark and gluons distributions from the $|y| < 2.1$ rapidity interval are shown in Fig. 1. The values of n extracted from the pure power-law fits are listed in Table 1. The power-law function can describe the gross-features of the spectra but the ratios of the spectra to the fit functions presented in the bottom of the figure indicate significant deviations of the jet spectra from the power-law form.

The power-law distribution can be improved by adding a logarithmic $p_{\mathrm{T}}^{\mathrm{jet}}$ dependence to the exponent producing an "extended power-law",

$$\frac{dn}{dp_{\mathrm{T}}^{\mathrm{jet}}} = A\left(\frac{p_{\mathrm{T0}}}{p_{\mathrm{T}}^{\mathrm{jet}}}\right)^{n+\beta\log\left(p_{\mathrm{T}}^{\mathrm{jet}}/p_{\mathrm{T0}}\right)}. \tag{2}$$

With this form, β represents the logarithmic derivative of $dn/dp_{\mathrm{T}}^{\mathrm{jet}}$ at $p_{\mathrm{T}}^{\mathrm{jet}} = p_{\mathrm{T0}}$. At the most forward rapidities, the strong phase-space suppression of the jet spectra at high $p_{\mathrm{T}}^{\mathrm{jet}}$ makes even the extended power-law inadequate for describing the jet spectra. Thus, for the most forward rapidities, an additional quadratic term, $\gamma \log^2\left(p_{\mathrm{T}}^{\mathrm{jet}}/p_{\mathrm{T0}}\right)$, is added to the power-law exponent and the resulting function is capable of describing the most forward quark and gluon spectra over the $p_{\mathrm{T}}^{\mathrm{jet}}$ range used in this analysis.

A jet spectrum that consists of a mixture of quark and gluon contributions can be represented in terms of a sum of contributions each of the form of Eq. 1 or its extensions. However, for the purposes of this paper, it will be convenient to express the combined spectrum in terms of a quark fraction, f_{q0}, specified at p_{T0}. Then a combined spectrum using power-law forms can be written

$$\frac{dN}{dp_{\mathrm{T}}^{\mathrm{jet}}} = A\left[f_{q0}\left(\frac{p_{\mathrm{T0}}}{p_{\mathrm{T}}^{\mathrm{jet}}}\right)^{n_q} + (1-f_{q0})\left(\frac{p_{\mathrm{T0}}}{p_{\mathrm{T}}^{\mathrm{jet}}}\right)^{n_g}\right], \quad (3)$$

where n_q and n_g are the quark and gluon power-law indices, respectively. Since $n_q \neq n_g$, the quark fraction will evolve as a function of $p_{\mathrm{T}}^{\mathrm{jet}}$ according to

$$f_q\left(p_{\mathrm{T}}^{\mathrm{jet}}\right) = \frac{f_{q0}\left(\frac{p_{\mathrm{T0}}}{p_{\mathrm{T}}^{\mathrm{jet}}}\right)^{n_q}}{f_{q0}\left(\frac{p_{\mathrm{T0}}}{p_{\mathrm{T}}^{\mathrm{jet}}}\right)^{n_q} + (1-f_{q0})\left(\frac{p_{\mathrm{T0}}}{p_{\mathrm{T}}^{\mathrm{jet}}}\right)^{n_g}} = \frac{1}{1+\left(\frac{1-f_{q0}}{f_{q0}}\right)\left(\frac{p_{\mathrm{T0}}}{p_{\mathrm{T}}^{\mathrm{jet}}}\right)^{n_g-n_q}}. \quad (4)$$

For the extended power-law parameterizations of the spectra, the $p_{\mathrm{T}}^{\mathrm{jet}}$-dependent quark fraction looks similar to that in Eq. 4 but with the addition of a term, $(\beta_g - \beta_q)\log\left(p_{\mathrm{T}}^{\mathrm{jet}}/p_{\mathrm{T0}}\right)$ to the exponent in the denominator. The $p_{\mathrm{T}}^{\mathrm{jet}}$ dependence of the quark fraction is shown in Fig. 2.

The PYTHIA8 $D(z)$ distributions were obtained using final-state charged hadrons located within an angular radius, $\Delta R < 0.4$, of reconstructed jets having $p_{\mathrm{T}}^{\mathrm{jet}} > 100$ GeV. The resulting distributions are shown in Fig. 3 for the rapidity interval $|y| < 2.1$. The quark $D(z)$ distribution is noticeably harder than the gluon $D(z)$ distribution, but is also lower at intermediate z, in the range where the $D(z)$ distribution appears to be depleted in Pb+Pb collisions.

For use in the analytic analysis, the $D(z)$ distributions were fit to functions of the form,

$$D(z) = a \cdot \frac{(1+dz)^b}{(1+ez)^c} \cdot \exp(-fz) \quad (5)$$

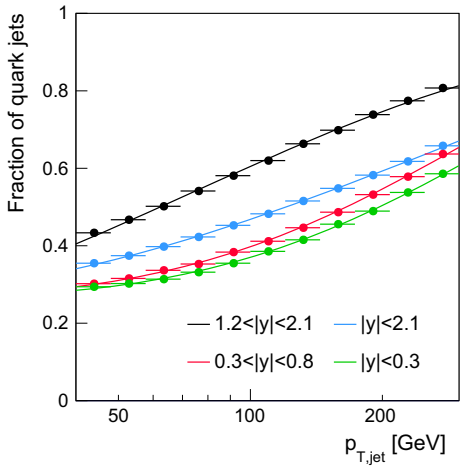

Fig. 2 Jet quark fraction as a function of $p_{\mathrm{T}}^{\mathrm{jet}}$ in the different jet rapidity intervals used in this study. The *points* show results obtained from PYTHIA8 simulations, the *solid lines* represent results obtained from extended power-law fits with the parameters shown in Table 1

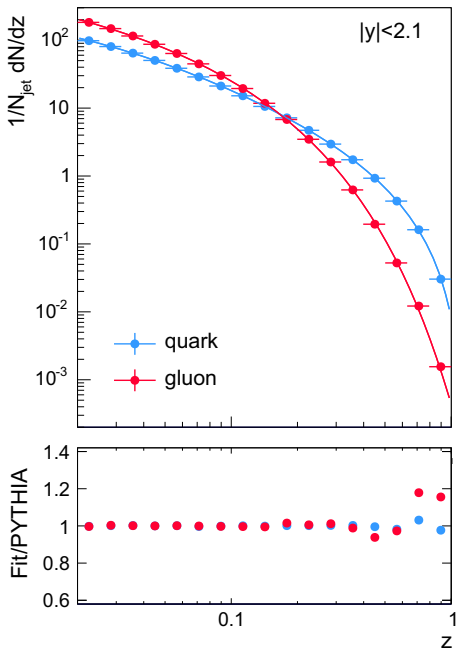

Fig. 3 PYTHIA8 quark and gluon $D(z)$ distributions for $R = 0.4$ jets having $p_{\mathrm{T}}^{\mathrm{jet}} > 100$ GeV and $|y| < 2.1$. The *solid lines* show the results of fits to the $D(z)$ distributions using the function in Eq. 5

which are similar to other commonly used parameterizations [26] with the addition of an exponential term. That term is not used for the quark distributions, but it's presence provides a more controlled description of the gluon $D(z)$ distribution. The results of the fits for the quark and gluon distributions over $|y| < 2.1$ are shown in Fig. 3, and the ratios of the fit to the PYTHIA8 $D(z)$ distributions are shown in the lower panels. The fits well describe the simulated $D(z)$ distributions with parameters that are provided in Table 2. We note

Table 2 Parameters describing the fragmentation functions extracted from PYTHIA8 using the procedures described in the text for the functional form in Eq. 5

	a	b	c	d	e	f
Quark	318	2.51	1.44	−0.85	52.4	0
Gluon	574	1.87	2.32	9.09	32.0	10.3

that the parameterization in Eq. 5 has a smooth extrapolation past $z = 1$. The pQCD fragmentation function has no contribution from $z > 1$, but when reconstructing jets in PYTHIA8 and data, there are events having two jets that are close enough that a high-$p_{\mathrm{T}}^{\mathrm{ch}}$ fragment from the higher-energy jet can be associated with the lower-energy jet possibly yielding a hadron with $z > 1$. The $D(z)$ distributions fall rapidly above $z = 1$ so they have no practical importance, though the continuity of the parameterization will be relevant later in this paper.

3 Analytic models for jet R_{AA} and $D(z)$: power-law spectra

Our modeling of the single jet suppression is based on the "shift" approach of [27] in which the quenched jet spectrum can be (approximately) written

$$\frac{dn_{\mathrm{Q}}(p_{\mathrm{T}}^{\mathrm{jet}})}{dp_{\mathrm{T}}^{\mathrm{jet}}} = \frac{dn\left(p_{\mathrm{T}}^{\mathrm{jet}} + S(p_{\mathrm{T}}^{\mathrm{jet}})\right)}{dp_{\mathrm{T}}^{\mathrm{jet}}} \times \left(1 + \frac{dS}{dp_{\mathrm{T}}^{\mathrm{jet}}}\right), \tag{6}$$

where dn_{Q} and dn represent the per-event yields of quenched and unquenched jets. The second term in Eq. 6 is a Jacobian term that is necessary to (e.g.) preserve the total number of jets.

Using the power-law form for a single-flavor jet spectrum,

$$\frac{dn_{Q}(p_{\mathrm{T}}^{\mathrm{jet}})}{dp_{\mathrm{T}}^{\mathrm{jet}}} = A\left(\frac{p_{\mathrm{T0}}}{p_{\mathrm{T}}^{\mathrm{jet}} + S(p_{\mathrm{T}}^{\mathrm{jet}})}\right)^{n}\left(1 + \frac{dS}{dp_{\mathrm{T}}^{\mathrm{jet}}}\right). \tag{7}$$

The ratio of the quenched and unquenched spectra, the analog of the measured R_{AA}, is then

$$R_{\mathrm{AA}}(p_{\mathrm{T}}^{\mathrm{jet}}) = \left(\frac{1}{1 + S(p_{\mathrm{T}}^{\mathrm{jet}})/p_{\mathrm{T}}^{\mathrm{jet}}}\right)^{n}\left(1 + \frac{dS}{dp_{\mathrm{T}}^{\mathrm{jet}}}\right). \tag{8}$$

It has been previously observed [28][1] that if the shift is proportional to $p_{\mathrm{T}}^{\mathrm{jet}}$, $S \equiv sp_{\mathrm{T}}$, then the resulting R_{AA} is $p_{\mathrm{T}}^{\mathrm{jet}}$-independent:

$$R_{\mathrm{AA}}(p_{\mathrm{T}}^{\mathrm{jet}}) = \frac{1}{(1+s)^{n-1}}, \tag{9}$$

such that the fractional shift can be inferred from an approximately $p_{\mathrm{T}}^{\mathrm{jet}}$-independent R_{AA} [28]

$$s = \frac{1}{R_{\mathrm{AA}}^{\left(\frac{1}{n-1}\right)}} - 1. \tag{10}$$

This result has previously been applied to single hadron R_{AA} measurements but is arguably more appropriate when applied to jet R_{AA} measurements. Then, naively applying Eq. 10 to the typical suppression observed at high $p_{\mathrm{T}}^{\mathrm{jet}}$ in central Pb+Pb collisions at the LHC, $R_{\mathrm{AA}} \sim 0.5$, and using $n \sim 5$, the resulting fractional shift would be $s = 0.19$. The observation that the jet R_{AA} is only weakly dependent on $p_{\mathrm{T}}^{\mathrm{jet}}$ at high $p_{\mathrm{T}}^{\mathrm{jet}}$ has been taken as evidence that jets lose a constant fraction of their energy in the quark gluon plasma created in Pb+Pb collisions. There are potentially significant theoretical flaws with this conclusion, but the conclusion and the interpretation of the extracted s also suffer from neglecting the fact that the jet spectrum is composed of an admixture of flavors.

Starting with a combination of quark and gluon power-law spectra (Eq. 3), the quenched spectrum would be

$$\frac{dN_{\mathrm{Q}}}{dp_{\mathrm{T}}^{\mathrm{jet}}} = A\left[f_{q0}\left(\frac{p_{\mathrm{T0}}}{p_{\mathrm{T}}^{\mathrm{jet}} + S_q}\right)^{n_q}\left(1 + \frac{dS_q}{dp_{\mathrm{T}}^{\mathrm{jet}}}\right) + \left(1 - f_{q0}\right)\left(\frac{p_{\mathrm{T0}}}{p_{\mathrm{T}}^{\mathrm{jet}} + S_g}\right)^{n_g}\left(1 + \frac{dS_g}{dp_{\mathrm{T}}^{\mathrm{jet}}}\right)\right]. \tag{11}$$

The resulting R_{AA} would be given by the ratio of Eqs. 11–3 which, with some simplification, takes the form

$$R_{\mathrm{AA}} = f_q\left(\frac{1}{1 + S_q/p_{\mathrm{T}}^{\mathrm{jet}}}\right)^{n_q}\left(1 + \frac{dS_q}{dp_{\mathrm{T}}^{\mathrm{jet}}}\right) + \left(1 - f_q\right)\left(\frac{1}{1 + S_g/p_{\mathrm{T}}^{\mathrm{jet}}}\right)^{n_g}\left(1 + \frac{dS_g}{dp_{\mathrm{T}}^{\mathrm{jet}}}\right). \tag{12}$$

Here, f_{q} is the full $p_{\mathrm{T}}^{\mathrm{jet}}$-dependent quark fraction in Eq. 4. As the equation indicates, the combined jet R_{AA} is given by a combination of the separate quark and gluon suppression factors weighted by the quark and gluon fractions.

Even in the case of constant fractional energy loss for the quarks and gluons, $S_q = s_q p_{\mathrm{T}}^{\mathrm{jet}}$ and $S_g = s_g p_{\mathrm{T}}^{\mathrm{jet}}$, Eq. 12 would imply an R_{AA} that varies with $p_{\mathrm{T}}^{\mathrm{jet}}$ as long as $S_q \neq S_g$. For example, if $S_g/S_q > 1$, then the R_{AA} will increase with $p_{\mathrm{T}}^{\mathrm{jet}}$ because of an increasing quark fraction and weaker suppression for the quarks. Such an increase of R_{AA} with increasing $p_{\mathrm{T}}^{\mathrm{jet}}$ has been observed in the measured R_{AA} values that

[1] The definition of n differs between this paper and [28] where it characterizes the invariant cross-section and is, therefore, larger by one due to the dp_{T}^2 factor.

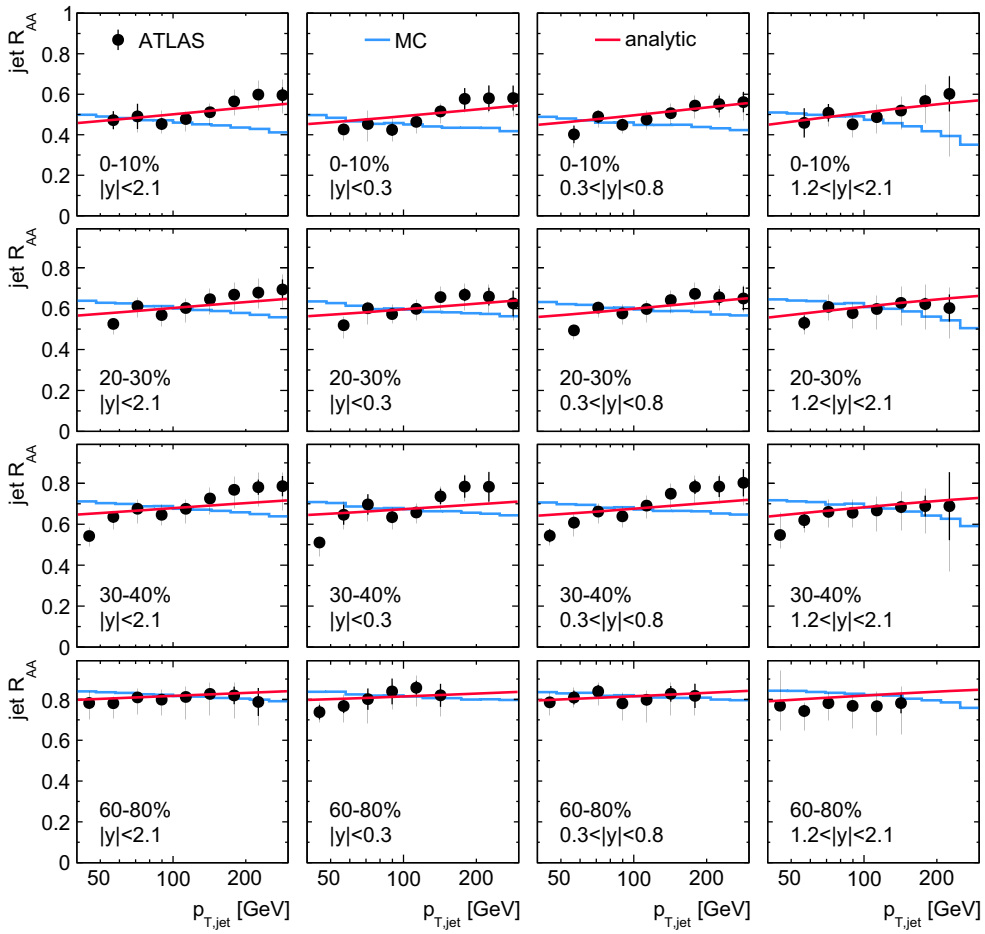

Fig. 4 Nuclear modification factor of jets, R_{AA}, measured by ATLAS [11] (*black markers*) in four different centrality bins (*rows*) and four different rapidity regions (*columns*) compared to the analytic calculation (*red line*) and MC calculation (*blue histogram*) of the R_{AA} using constant fractional shift and power-law spectra

are shown in Fig. 4. To test whether the data are compatible with the constant fractional energy loss scenario, we have assumed $s_g = 9/4 \times s_q$ and have fit the R_{AA} values using Eq. 12 with one free parameter for each centrality bin, namely s_q. The results are shown in Fig. 4 with solid lines. The extracted s_q values vary from 0.02 for the 60–80 % centrality bin to 0.1 for the 0–1 % bin. The figure shows that the constant fractional shift assumption combined with the power-law form for the jet spectra is capable of approximately reproducing the slow variation of the measured jet R_{AA} with $p_{\mathrm{T}}^{\mathrm{jet}}$.

Since the $p_{\mathrm{T}}^{\mathrm{jet}}$ dependence of the jet suppression can be successfully explained using a combination of the varying quark fraction and the greater quenching of gluon jets, it is worth exploring the impact of these same behaviors on the jet fragmentation function. In particular, we wish to determine whether the different quenching of the quarks and gluons can explain part or all of the the observed modifications of the fragmentation function in Pb+Pb collisions. We make the simplest possible assumption, namely that the quarks and gluons lose energy in the plasma and then fragment according to vacuum fragmentation functions. With this assumption, the only source of modification to the inclusive jet fragmentation function is the change in the quark (or gluon) fraction due to the medium-induced energy loss. Starting from Eq. 11, the modified quark fraction in the constant fractional shift scenario is

$$f_q^{\mathrm{mod}} = \frac{1}{1 + \left(\frac{1-f_{q0}}{f_{q0}}\right) \frac{\left(1+s_g\right)^{n_g-1}}{\left(1+s_q\right)^{n_q-1}} \left(\frac{p_{\mathrm{T}0}}{p_{\mathrm{T}}^{\mathrm{jet}}}\right)^{n_g-n_q}}. \tag{13}$$

Assuming that the $D(z)$ distributions are independent of $p_{\mathrm{T}}^{\mathrm{jet}}$, the per-jet distribution of fragments as a function of the fragment longitudinal momentum fraction, $D(z)$, can be written,

$$D(z) = f_q^{\mathrm{int}} D_q(z) + (1 - f_q^{\mathrm{int}}) D_g(z), \tag{14}$$

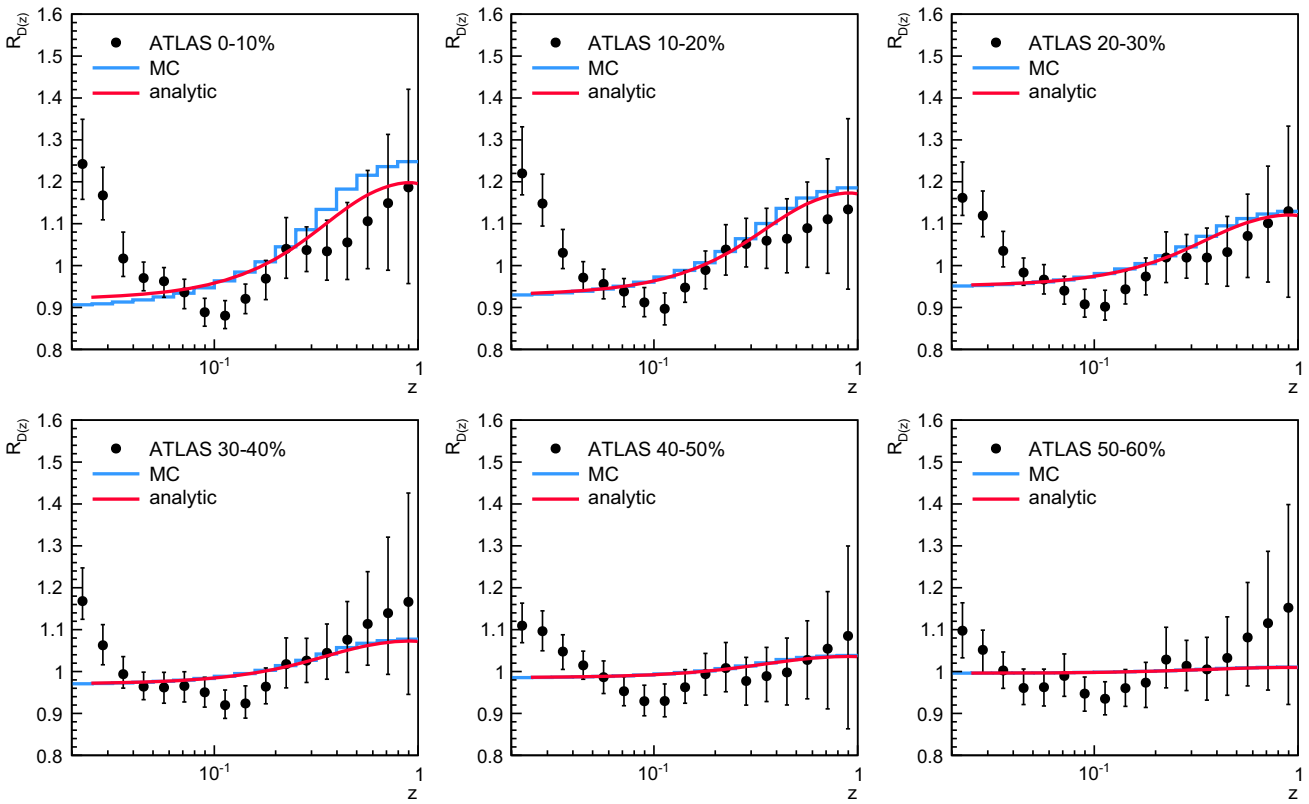

Fig. 5 Ratios of $D(z)$ distributions for six bins in collision centrality to those in peripheral (60–80 %) collisions, $D(z)|_{\text{cent}}/D(z)|_{60-80}$, measured by ATLAS for $R = 0.4$ jets [12] (*black markers*) are compared to the analytic calculation (*red line*) and MC calculation (*blue histogram*) of the same quantity in the fractional energy loss model. The analytic calculation uses the power law parameterization of jet p_{T} spectra

where $D_q(z)$ and $D_g(z)$ are the quark and gluon $D(z)$ distributions, respectively, and f_q^{int} is the modified quark fraction integrated over a given $p_{\text{T}}^{\text{jet}}$ range.

The ATLAS jet fragmentation measurements were obtained for $p_{\text{T}}^{\text{jet}} > 100$ GeV. Applying Eq. 14 over this $p_{\text{T}}^{\text{jet}}$ range and using the s_q parameters obtained from fits to the jet R_{AA}, we calculated the ratio of modified $D(z)$ distributions in different centrality bins to the distribution in the 60–80 % centrality bin for comparison with the ATLAS data. The results are shown along with the data in Fig. 5. The figure shows that our simple model for the medium modifications of the inclusive jet fragmentation function can reproduce some of the qualitative features in the data, namely the suppression of the fragmentation function at intermediate z and an enhancement in the fragmentation function at large z. This latter is statistically marginal in the data given the (combined) error bars, but the enhancement at large z in the model is an automatic result of the increased quark content of the jet spectrum. Our model does not show as deep a suppression in the $D(z)$ ratio near 0.1 which may indicate that additional physics contributes there.

One feature in the data that cannot be explained by the model is the enhancement at low z. Our simple model also explains the centrality dependence of the data, except for the 50–60 % centrality bin, given the fits to the single-jet suppression. Based on the results shown in Fig. 5 we argue that it is plausible that the modifications observed at intermediate and large z in the jet fragmentation function result from quenching-driven changes in the jet quark fraction while the enhancement at low z reflects a contribution of extra particles in the jet either from radiative emission within the jet or recoil of particles in the medium.

We have performed a separate Monte-Carlo evaluation of the single-jet suppression to check and improve on the results of the above analytic calculations which are necessarily limited by assumptions regarding the shapes of the jet spectra. To simulate the single-jet suppression, we sample jets from the PYTHIA8-simulated events, apply the shift as in Eq. 6 with chosen S_q and S_g for quark and gluon jets, respectively, and then build the resulting spectra of quenched jets. The simulated R_{AA} is obtained from the ratio of the quenched spectrum to the original spectrum of PYTHIA8 jets. The results are shown with the blue histograms in Fig. 4. The agreement with the analytic results is poor, suggesting that the power-law parameterization of the jet spectra is inadequate for the simulation of the single-jet suppression. In fact, the

Monte-Carlo sampled $R_{\rm AA}$ decreases with increasing $p_{\rm T}^{\rm jet}$ in contradiction with the general result that constant fractional shift combined with the increasing quark fraction should produce an $R_{\rm AA}$ that increases with $p_{\rm T}^{\rm jet}$. The decrease of the Monte-Carlo sampled $R_{\rm AA}$ must necessarily result from the jet spectra being steeper, or having greater curvature than the power-law function or, equivalently, from the differences between the power-law fit functions and the PYTHIA8 spectra seen in Fig. 1.

4 Analytic models for jet $R_{\rm AA}$: extended power-law spectra

To test this conclusion, we have extended the analytic analysis from the previous section to the case of extended power-law spectra. The analog of Eq. 7 is

$$\frac{dn_{\rm Q}}{dp_{\rm T}^{\rm jet}} = A\left(\frac{p_{\rm T0}}{p_{\rm T}^{\rm jet}+S}\right)^{n+\beta\log\left[(p_{\rm T}^{\rm jet}+S)/p_{\rm T0}\right]}\left(1+\frac{dS}{dp_{\rm T}^{\rm jet}}\right), \tag{15}$$

and the $R_{\rm AA}$ is:

$$R_{\rm AA} = \left(1+\frac{dS}{dp_{\rm T}^{\rm jet}}\right)\left(\frac{p_{\rm T0}}{p_{\rm T}^{\rm jet}}\right)^{2\beta\log\left(1+S/p_{\rm T}^{\rm jet}\right)} \times\left(\frac{1}{1+S/p_{\rm T}^{\rm jet}}\right)^{n+\beta\log\left(1+S/p_{\rm T}^{\rm jet}\right)}. \tag{16}$$

The logarithmic term in the exponent of the extended power-law function not only produces a corresponding logarithmic term in the exponent of $1/(1+S/p_{\rm T}^{\rm jet})$ but it also generates an explicit dependence on $p_{\rm T0}/p_{\rm T}^{\rm jet}$. Thus, even for a constant fractional shift, the $R_{\rm AA}$ decreases with increasing $p_{\rm T}^{\rm jet}$ for positive β:

$$R_{\rm AA} = \left(\frac{p_{\rm T0}}{p_{\rm T}^{\rm jet}}\right)^{2\beta\log(1+s)}\left(\frac{1}{1+s}\right)^{n-1+\beta\log(1+s)}. \tag{17}$$

For a spectrum consisting of both quarks and gluons, the $R_{\rm AA}$ is given by an expression similar to Eq. 12 containing an f_q- and $(1-f_q)$-weighted combinations of Eq. 15 with different values for n and β for quarks and gluons (full equations are provided in the "Appendix"). Given the f_q distributions in Fig. 2, a constant fraction shift is unable to reproduce the measured increase of the jet $R_{\rm AA}$ with increasing $p_{\rm T}^{\rm jet}$. In fact, a calculation of the $R_{\rm AA}$ using the extended power-law form well reproduces the results of the Monte Carlo evaluation shown in Fig. 4. Thus, we conclude that the apparent success of the constant fractional shift scenario in Fig. 4 using the analytic analysis is false and results from neglecting the deviations of the jet spectra from the pure power-law form.

5 Modeling jet $R_{\rm AA}$ and $D(z)$: non-constant fractional shift

The inability of the constant fractional shift assumption to explain the $p_{\rm T}^{\rm jet}$ dependence of the measured $R_{\rm AA}$ suggests that the shift has to vary with $p_{\rm T}^{\rm jet}$ more slowly than linearly. In fact, theoretical analyses of medium-induced energy loss would not be compatible with a constant fractional shift scenario. To proceed, we make the minimal extension of the analysis above and assume that the shift is proportional to an undetermined power of $p_{\rm T}^{\rm jet}$,

$$S = s'\left(\frac{p_{\rm T}^{\rm jet}}{p_{\rm T0}}\right)^{\alpha}. \tag{18}$$

Lacking any knowledge of the appropriate scale for the term in the parenthesis, we use the same reference scale, $p_{\rm T0}$, used for parameterizing the spectra. Then, s', which has dimensions of energy or transverse momentum, represents the shift in transverse momentum for jets having $p_{\rm T}^{\rm jet} = p_{\rm T0}$. The resulting $R_{\rm AA}$ for a single jet spectrum and for combined quark and gluon spectra can be obtained using the procedures described above, in particular a combination of Eq. 15 weighted by the $p_{\rm T}^{\rm jet}$-dependent quark and gluon fractions; the formulas are not shown here for sake of brevity.

The shift expression in Eq. 18 and the resulting $R_{\rm AA}$ were used to perform a fit to the ATLAS data to extract s' and α in different centrality bins. The fits were performed using the statistical uncertainties in the χ^2. The results are presented in Fig. 6 where the top panels show χ^2 contours in s'–α space for the 10–20 % (left) and 70–80 % (right) centrality bins. As the contours demonstrate, there is a strong correlation between the parameters which causes the obtained optimal α and s' values, shown in the lower panels of the figure as a function of $N_{\rm part}$, to fluctuate. The α values, however, cluster around an average value of 0.55. To reduce the point-to-point scatter in the obtained parameters α was fixed to the value 0.55 and the fits were run again to extract s'. The values are shown in the lower right panel with the red points. The white and black circles shown on the χ^2 contour plots indicate, respectively the results of the free fits and the fits with $\alpha = 0.55$.

The s' values obtained using fixed α show an approximately linear dependence on $N_{\rm part}$ and vary from ~1 GeV in the most peripheral bin to ~5.5 GeV in the most central (0–1 %) bin. The fact that s' extrapolates to a non-zero value for $N_{\rm part} \to 0$ may indicate that there is an additional contri-

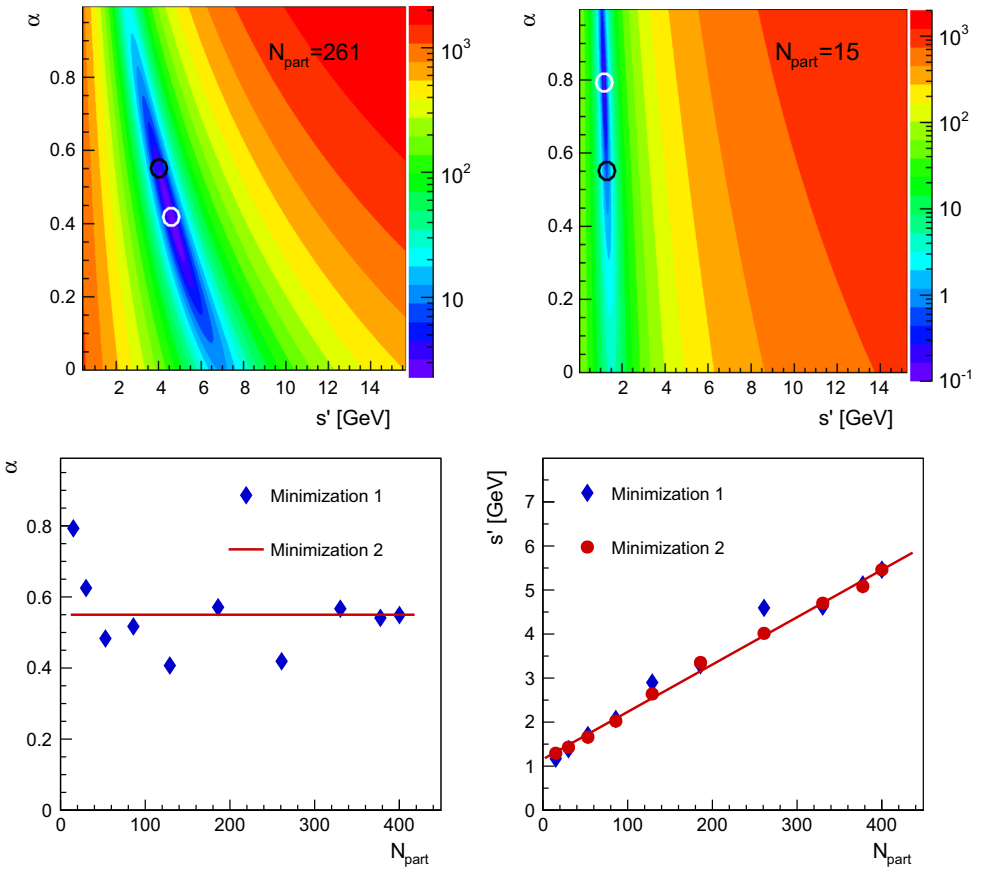

Fig. 6 *Top* χ^2/DOF as a function of α and s' for the 10–20 % (*left*) and 70–80 % (*right*) centrality bins. The positions of the minima with α free (fixed) are indicated by the *white* (*black*) *circles*. *Bottom* parameters of non-fractional shift (Eq. 18) model, α (*left*) and s' (*right*), as a function of N_{part} obtained from fits of the resulting calculated R_{AA} to the ATLAS data. The *blue points* indicate results for which both α and s' are free parameters while the *red points* indicate the results of fits with α fixed to 0.55 (see text) shown on the *left panel by the red line*. The *line on the right panel* shows the result of a linear fit to $s'(N_{\text{part}})$

bution to the measured single-jet suppression present in even peripheral collisions. In fact, the free fits suggest a systematic rise in α for the two most peripheral bins which may arise from the same underlying physics.

The R_{AA} calculated using the results of the fitting procedure are shown in Fig. 7. Using the extended power-law parameterization of the quark and gluon spectra, the analytic and Monte Carlo results are in good agreement. The growth of the R_{AA} with $p_{\text{T}}^{\text{jet}}$ results from the fact that the shift increases with $p_{\text{T}}^{\text{jet}}$ more slowly than linearly. Thus, the fractional energy loss decreases with increasing $p_{\text{T}}^{\text{jet}}$. The agreement with the data is largely by construction since the parameters of the energy loss were obtained from the above-described fitting procedure. Nonetheless, our model is capable of describing the available data with a single, centrality-independent value for α and a proportionality constant, s' that varies approximately linearly with N_{part}.

The rapidity dependence, or lack thereof, in the R_{AA} arises from a cancellation between the rapidity dependence of the quark fraction, which increases with increasing rapidity (see Fig. 2), and the shapes of the quark and gluon spectra which become steeper with increasing rapidity. This cancellation is illustrated in Fig. 8 which shows the suppression for the quark, gluon, and combined spectra in the $|y| < 0.3$ (left) and $1.2 < |y| < 2.1$ (right) rapidity bins. The difference between the quark and gluon suppression is greater in the $1.2 < |y| < 2.1$ than in the $|y| < 0.3$ bin. The $p_{\text{T}}^{\text{jet}}$ dependence is also much flatter in the higher rapidity bin. Yet, the combined suppression taking into account the $p_{\text{T}}^{\text{jet}}$ dependence of f_{q} in Fig. 2 is nearly the same in the two rapidity bins.

The $D(z)$ distributions calculated using the extended power-law functions and the shift in Eq. 18 are shown in Fig. 9. As with the R_{AA}, the agreement between the analytic calculation and the Monte-Carlo sampled result is much better using the extended power-law descriptions of the primordial parton spectra. However, the $D(z)$ modifications in the model are largely the same using the fractional and non-fractional shift parameterizations. This lack of sensitivity to $S(p_{\text{T}}^{\text{jet}})$ arises because the $D(z)$ measurements are dominated by contributions from jets with $p_{\text{T}}^{\text{jet}} \sim 100$ GeV and because

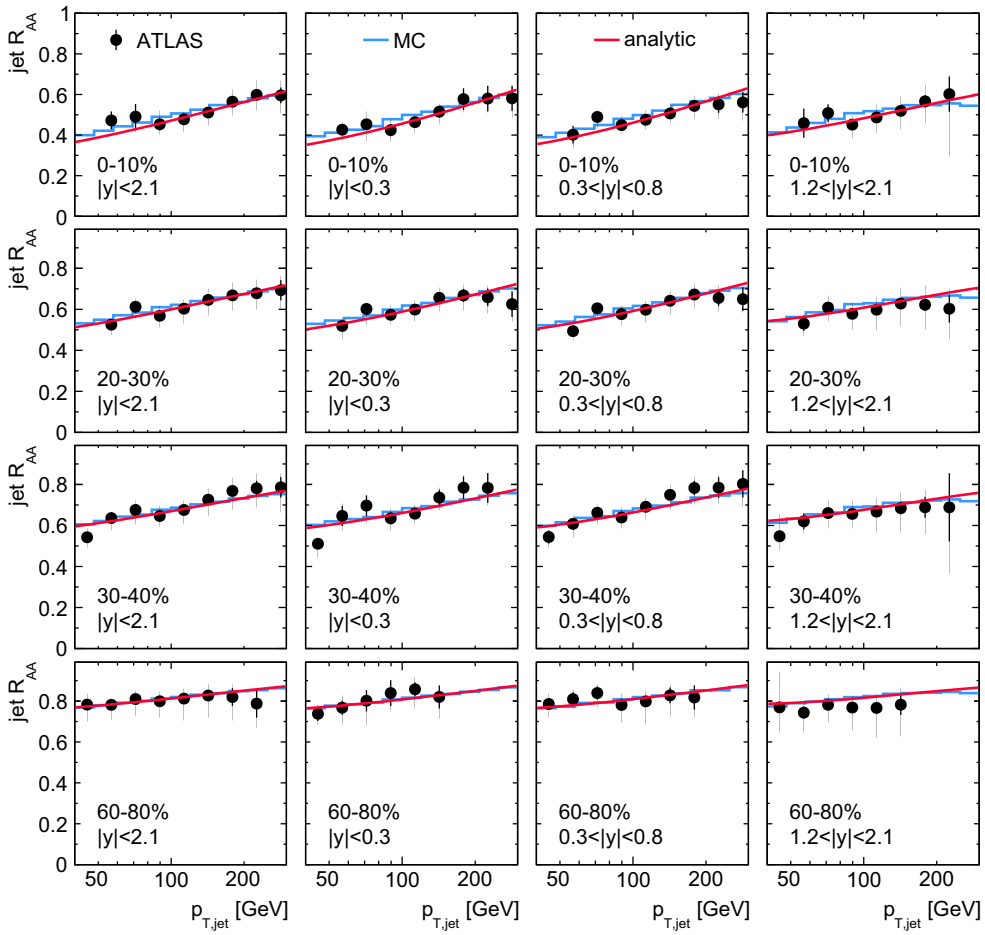

Fig. 7 Nuclear modification factor of jets, R_{AA}, measured by ATLAS [11] (*black markers*) in four different centrality bins (*rows*) and four different rapidity regions (*columns*) is compared to the analytic calculation (*red line*) and MC calculation (*blue histogram*) of the same quantity in the non-constant fractional energy loss model. The analytic calculation uses the extended power law parameterization of the jet p_{T} spectra that includes the logarithmic dependence of the exponent on jet p_{T}

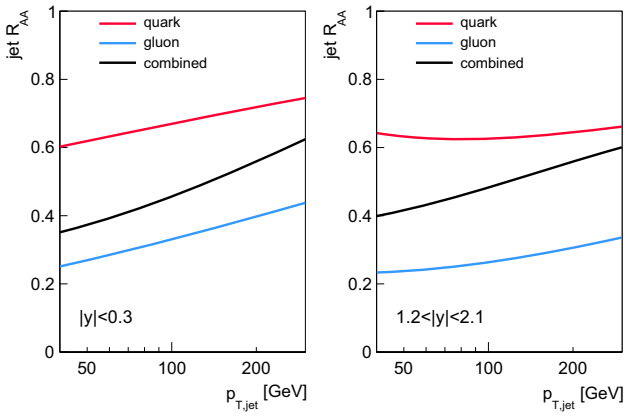

Fig. 8 Quark, gluon, and combined R_{AA} vs $p_{\mathrm{T}}^{\mathrm{jet}}$ for the $|y| < 0.3$ (*left*) and $1.2 < |y| < 2.12$ (*right*) rapidity bins

the $D(z)$ modifications in the model primarily result from the difference between quark and gluon quenching for jets with similar transverse momenta. Thus, as long as the model reproduces the R_{AA} near 100 GeV the $D(z)$ modifications will be insensitive to the $p_{\mathrm{T}}^{\mathrm{jet}}$ dependence of S.

6 Rapidity dependence of the suppression

The fraction of jets initiated by light quarks evolves as a function of the rapidity such that the probability that the jet is initiated by a quark is increasing with increasing rapidity. The steepness of the jet p_{T} spectrum also evolves as a faction of the rapidity such that the p_{T} spectra of forward jets are steeper than the spectra of jets produced in the central region. Both of these features are demonstrated in Fig. 2 and Table 1 of Sect. 2. Both features also influence the jet R_{AA}, though they act in opposite directions. Nonetheless, it can reasonably be expected that the jet R_{AA} will exhibit a different behavior in the forward region compared to the central region, or, equivalently, that the R_{AA} will vary with rapidity at sufficiently large values. Thus, it is clearly of interest to test

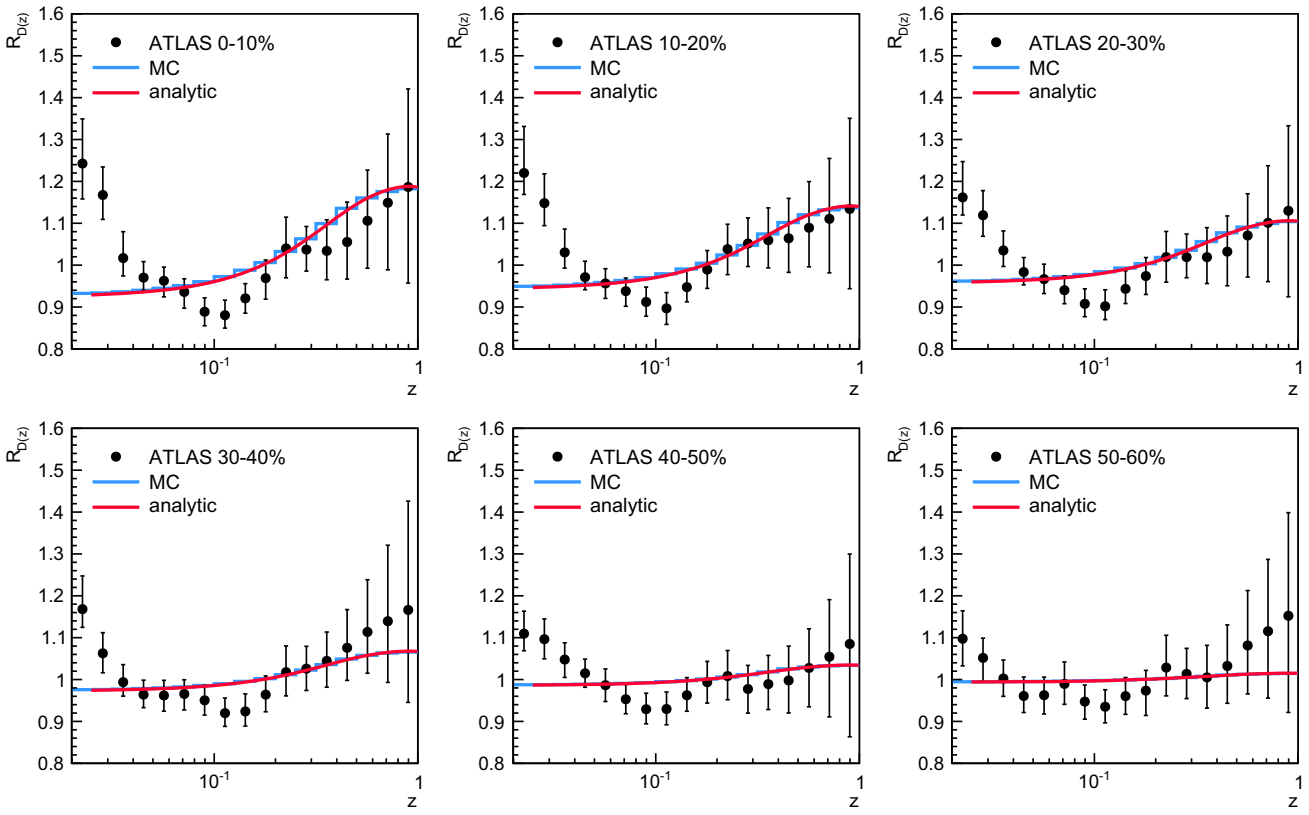

Fig. 9 Ratios of $D(z)$ distributions for six bins in collision centrality to those in peripheral (60–80 %) collisions, $D(z)|_{\text{cent}}/D(z)|_{60-80}$, measured by ATLAS for $R = 0.4$ jets [12] (*black markers*) are compared to the analytic calculation (*red line*) and MC calculation (*blue histogram*) of the same quantity in the non-constant fractional energy loss model

the model presented in this paper by predicting the jet R_{AA} in the forward region where it has not yet been measured. To do that, the jet R_{AA} was calculated using the analytic model in two bins of jet rapidity corresponding to those used by ATLAS or CMS [29,30], namely $2.1 < |y| < 2.8$ and $2.8 < |y| < 3.5$. In the later rapidity region, the jet p_{T} spectra decrease approximately by four orders of magnitude in the region of jet p_{T} between 40 and 100 GeV. This steep fall-off of the spectra was found to be insufficiently described by the modified power-law, Eq. 2. To improve the parameterization, an additional quadratic term was introduced leading to the parameterization,

$$\frac{dn}{dp_{\text{T}}^{\text{jet}}} = A\left(\frac{p_{\text{T0}}}{p_{\text{T}}^{\text{jet}}}\right)^{n+\beta\log\left(p_{\text{T}}^{\text{jet}}/p_{\text{T0}}\right)+\gamma\log^2\left(p_{\text{T}}^{\text{jet}}/p_{\text{T0}}\right)}, \quad (19)$$

which was found to describe the PYTHIA jet p_{T} spectra at the level of accuracy better then 10 %. The resulting parameters and the quark fractions for the jet p_{T} spectra selected in the two rapidity regions are summarized in Table 3.

The resulting analytic R_{AA} was calculated using an extension of Eq. 16 to account for the quadratic term, and using the results from Sect. 3, namely a shift of the form of Eq. 18 with $\alpha = 0.55$ and $s'(N_{\text{part}})$ as shown in Fig. 6.

Table 3 Parameters obtained from fits of the PYTHIA8 forward jet spectra to the extended power-law (Eq. 19) forms

Parameter	$2.1 < \|y\| < 2.8$	$2.8 < \|y\| < 3.5$
n_q	5.5	6.7
n_g	6.3	7.4
β_q	0.34	−0.46
β_g	0.52	−1.19
γ_q	1.2	2.6
γ_g	1.5	2.4
f_q	0.60	0.76

The predicted forward R_{AA} is shown as a function of $p_{\text{T}}^{\text{jet}}$ in Fig. 10. A clear change in the trend of the R_{AA} evolution with jet p_{T} can be seen. In contrast to the slow increase seen for the jet R_{AA} in the rapidity regions within $|y| < 2.1$, the jet R_{AA} in the forward regions first increases, reaches a maximum and then decreases with increasing $p_{\text{T}}^{\text{jet}}$. The decrease is more pronounced for more forward region where the jet R_{AA}

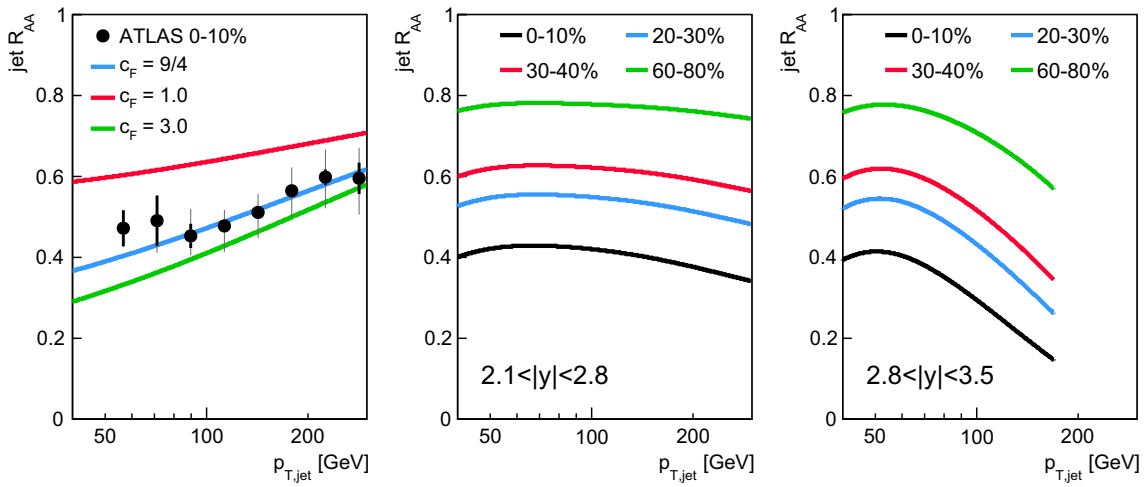

Fig. 10 *Left panel* ATLAS data on the jet R_{AA} in 0–10 % centrality bin (*black markers*) compared to the analytic calculation of the non-constant fractional energy loss for three different values of *color* factors: the default value of *color* factor $c_F = 9/4$ (*blue*), $c_F = 1.0$ (*red*), and $c_F = 3.0$ (*green*). *Middle panel* predicted jet R_{AA} as a function of $p_{\mathrm{T}}^{\mathrm{jet}}$ in forward rapidity interval $2.1 < |y| < 2.8$. *Right panel* predicted jet R_{AA} as a function of $p_{\mathrm{T}}^{\mathrm{jet}}$ in forward rapidity interval $2.8 < |y| < 3.5$. The R_{AA} predictions are shown for four centrality bins, 0–10 % (*black*), 20–30 % (*blue*), 30–40 % (*red*), and 60–80 % (*green*)

in 0–10 % central collisions reaches the maximum of approximately 0.4 at around 50 GeV, and then it decreases reaching a value of approximately 0.15 at 170 GeV. These trends are present across different centralities. Such pronounced change in the behavior of the forward jet R_{AA} represents a distinct feature that can be tested by future measurements at the LHC.

The dependence of the quark fraction on the jet rapidity has to influence also the trends measured in the centrality dependent ratios of fragmentation functions, $R_{D(z)}$, presented in Sect. 5. As demonstrated in Sect. 3, this ratio exhibits only a weak dependence on the shape of the underlying jet p_{T} spectra and thus, it is a very useful observable that may help isolate the effects of different quenching of quark-initiated and gluon-initiated jets. The sensitivity of the $D(z)$ modification to differences in quark and gluon quenching are illustrated in the left panel of Fig. 11 which shows $R_{D(z)}$ in 0–10 % central collisions evaluated for three different choices of an effective color factor, $c_F = 1.0, 9/4$, and 3.0. A clear dependence of the $R_{D(z)}$ on the color factor can be seen. For equal suppression of the quark-initiated and gluon-initiated jets, the $R_{D(z)}$ exhibits only negligible difference from unity reflecting minor difference in the quark fraction at unquenched and quenched jet transverse momenta. For color factor larger than the default value of 9/4, the $R_{D(z)}$ exhibits larger increase compared to the $R_{D(z)}$ evaluated with the default value of c_F.

The middle panel of Fig. 11 shows the $R_{D(z)}$ evaluated in 0–10 % central collisions for the rapidity region $|y| < 2.1$ and the prediction for the rapidity dependence of the $R_{D(z)}$ for three rapidity regions chosen to match the rapidity regions used in the measurement of the jet R_{AA} by ATLAS [11], namely $|y| < 0.3$, $0.3 < |y| < 0.8$, and $1.2 < |y| < 2.1$. The differences in the $R_{D(z)}$ are better quantified in terms of the ratio of $R_{D(z)}$ evaluated in a given rapidity region to that evaluated in the region of $|y| < 2.1$ as shown in the right panel of Fig. 11. The ratio is predicted to reach larger values in the more central rapidity region and smaller values in more forward region compared to the inclusive rapidity interval. Both of these effects are in the maximum at the level of 6–7 % of the inclusive $R_{D(z)}$. This predicted behavior represents another possibility to test the model and, more generally, to probe the differences between the energy loss of quark and gluon jets.

7 Modeling $D(p_{\mathrm{T}})$ and charged particle R_{AA}

We have shown that our simple model for the medium modifications of single jets can reproduce the measured nuclear modification factor and its rapidity and transverse momentum dependence. The model can also reproduce some of the qualitative features seen in measured inclusive jet fragmentation functions, namely the suppression at intermediate z and an enhancement at large z. It was shown that these features in the measured fragmentation functions arise from the change in the quark (or gluon) fraction due to the medium-induced energy loss. Since the model can explain both the jet spectra and the fragmentation functions, it should be also able to reproduce the charged particle transverse momentum distribution, $D(p_{\mathrm{T}}^{\mathrm{ch}})$, of charged particles produced within jets, and the nuclear modification factor of charged particles, $R_{\mathrm{AA}}^{\mathrm{ch}}$, measured at high transverse momenta of charged

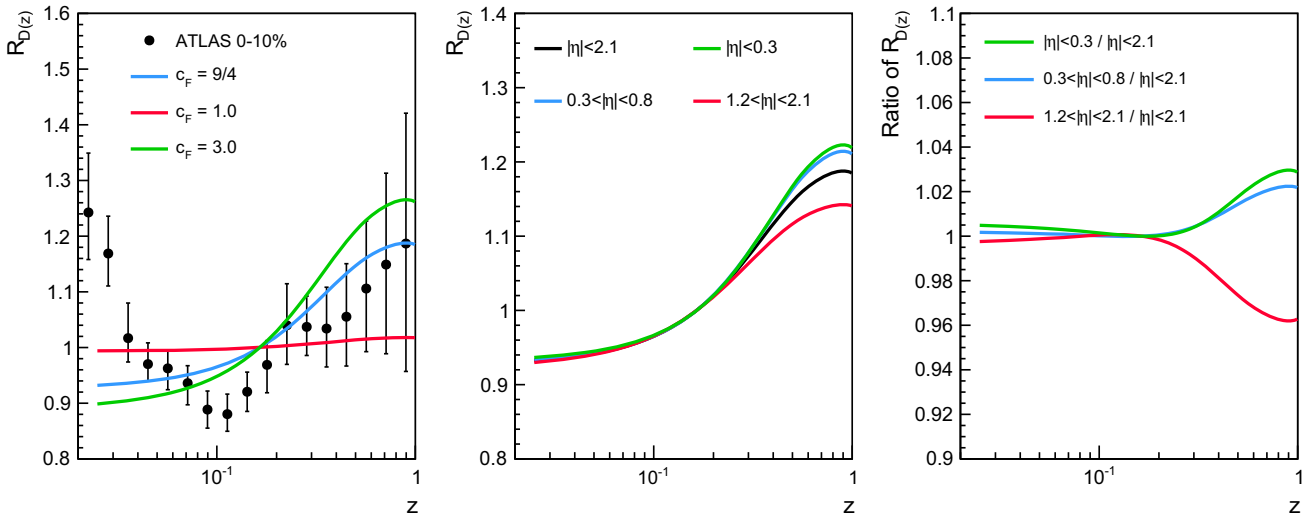

Fig. 11 *Left panel* ATLAS data on the ratio of $D(z)$ distributions, $R_{D(z)}$, in 0–10 to 60–80 % centrality bin (*black markers*) compared to the analytic calculation of the non-constant fractional energy loss for three different values of *color* factors: the default value of *color* factor $c_F = 9/4$ (*blue*), $c_F = 1.0$ (*red*), and $c_F = 3.0$ (*green*). *Middle panel* prediction of the ratio of $D(z)$ distributions, $R_{D(z)}$, in 0–10 to 60–80 % centrality bin in different jet rapidities. The $R_{D(z)}$ in the rapidity region of $|y| < 2.1$ (*black*) is compared to the $R_{D(z)}$ in the regions: $|y| < 0.3$ (*green*), $0.3 < |y| < 0.8$ (*blue*), and $1.2 < |y| < 2.1$ (*red*). *Right panel* the ratio of predicted $R_{D(z)}$ in different rapidity regions to the $R_{D(z)}$ in the region of $|y| < 2.1$

particles, $p_{\mathrm{T}}^{\mathrm{ch}}$. The $D(p_{\mathrm{T}}^{\mathrm{ch}})$ distributions were measured by ATLAS [12] and CMS [13] for jets with $p_{\mathrm{T}}^{\mathrm{jet}} > 100$ GeV. The charged particle $R_{\mathrm{AA}}^{\mathrm{ch}}$ at high $p_{\mathrm{T}}^{\mathrm{ch}}$ was measured by CMS [9]. Compared to the inclusive jet fragmentation functions which are largely independent of the jet transverse momentum for a given flavor of the initial parton, these observables couple together the change in the jet fragmentation and the change in the underlying jet spectra. Thus, these observables provide another important input to test the model.

The PYTHIA8 simulated events were used to simulate the modifications of the $D(p_{\mathrm{T}}^{\mathrm{ch}})$ distributions. The simulation was done in two steps. In the first step, the $D(p_{\mathrm{T}}^{\mathrm{ch}})$ distributions were booked in 1 GeV bins of the $p_{\mathrm{T}}^{\mathrm{jet}}$ to two look-up tables, for quark initiated and gluon initiated jets separately. In the second step, the jet suppression was applied at the single jet level in the same way as for the case of simulating the inclusive jet R_{AA}. For each suppressed jet of a given flavor, the $D(p_{\mathrm{T}}^{\mathrm{ch}})$ distribution corresponding to the quenched jet p_{T} was read off from the look-up table and added to the histogram which formed the resulting $D(p_{\mathrm{T}}^{\mathrm{ch}})$ distribution after being properly normalized by a total number of quenched jets with $p_{\mathrm{T}}^{\mathrm{jet}} > 100$ GeV. The central to peripheral ratio of $D(p_{\mathrm{T}}^{\mathrm{ch}})$ distributions, $R_{D(p_{\mathrm{T}}^{\mathrm{ch}})}$, was evaluated. The result is shown along with the data by ATLAS in Fig. 12. The figure shows that our model can reproduce the qualitative features observed in the data, namely the suppression of yields at intermediate $p_{\mathrm{T}}^{\mathrm{ch}}$ and an enhancement at high $p_{\mathrm{T}}^{\mathrm{ch}}$. This is not surprising given the success of the model in describing the $D(z)$ modifications, but it represents an important consistency check.

To evaluate the nuclear modification factor of charged particles, $R_{\mathrm{AA}}^{\mathrm{ch}}$, one can use the same procedure as for evaluating the $R_{D(p_{\mathrm{T}}^{\mathrm{ch}})}$ with only two differences which is evaluating the $D(p_{\mathrm{T}}^{\mathrm{ch}})$ distributions for jets with no threshold on jet p_{T} and avoiding a normalization of the final $D(p_{\mathrm{T}}^{\mathrm{ch}})$ distributions by the total number of jets. This approach is based on the fact that each charged particle with a given $p_{\mathrm{T}}^{\mathrm{ch}}$ must come from the jet with $p_{\mathrm{T}}^{\mathrm{jet}} \geq p_{\mathrm{T}}^{\mathrm{ch}}$. This allows to construct the $R_{\mathrm{AA}}^{\mathrm{ch}}$ for $p_{\mathrm{T}}^{\mathrm{ch}} > 20$ GeV which is the kinematic region where we have a good confidence in modeling the inclusive jet suppression. The resulting $R_{\mathrm{AA}}^{\mathrm{ch}}$ is shown along with the $R_{\mathrm{AA}}^{\mathrm{ch}}$ measured by CMS in Fig. 13.

The figure shows that the model can reproduce the qualitative features seen in the data at high-$p_{\mathrm{T}}^{\mathrm{ch}}$, namely the increase of the $R_{\mathrm{AA}}^{\mathrm{ch}}$ with increasing $p_{\mathrm{T}}^{\mathrm{ch}}$ and its centrality dependence. However, the slope of the charged particle R_{AA} in the model differs from that in the data at the lowest $p_{\mathrm{T}}^{\mathrm{ch}}$ values included in this analysis and the model systematically slightly over-predicts the $R_{\mathrm{AA}}^{\mathrm{ch}}$ in the data. These disagreements may be due to insufficient precision in the modeling of $D(p_{\mathrm{T}}^{\mathrm{ch}})$ distributions by PYTHIA8, something that can and will be tested in future analyses. There may be consequences from the disagreements between the data and the model in the $R_{D(z)}$ ($R_{D(p_{\mathrm{T}}^{\mathrm{ch}})}$) including the low-$z$ (low-$p_{\mathrm{T}}^{\mathrm{ch}}$) excess and fact that the data is systematically lower than the model in the range $0.1 < z < 0.2$ ($10 < p_{\mathrm{T}}^{\mathrm{ch}} < 20$ GeV). The former is discussed in the next section, the latter may be insufficient to explain the observed difference. Generally, the disagreement may be due to jet quenching physics not included in the model. In particular, the possibility that the jet quenching

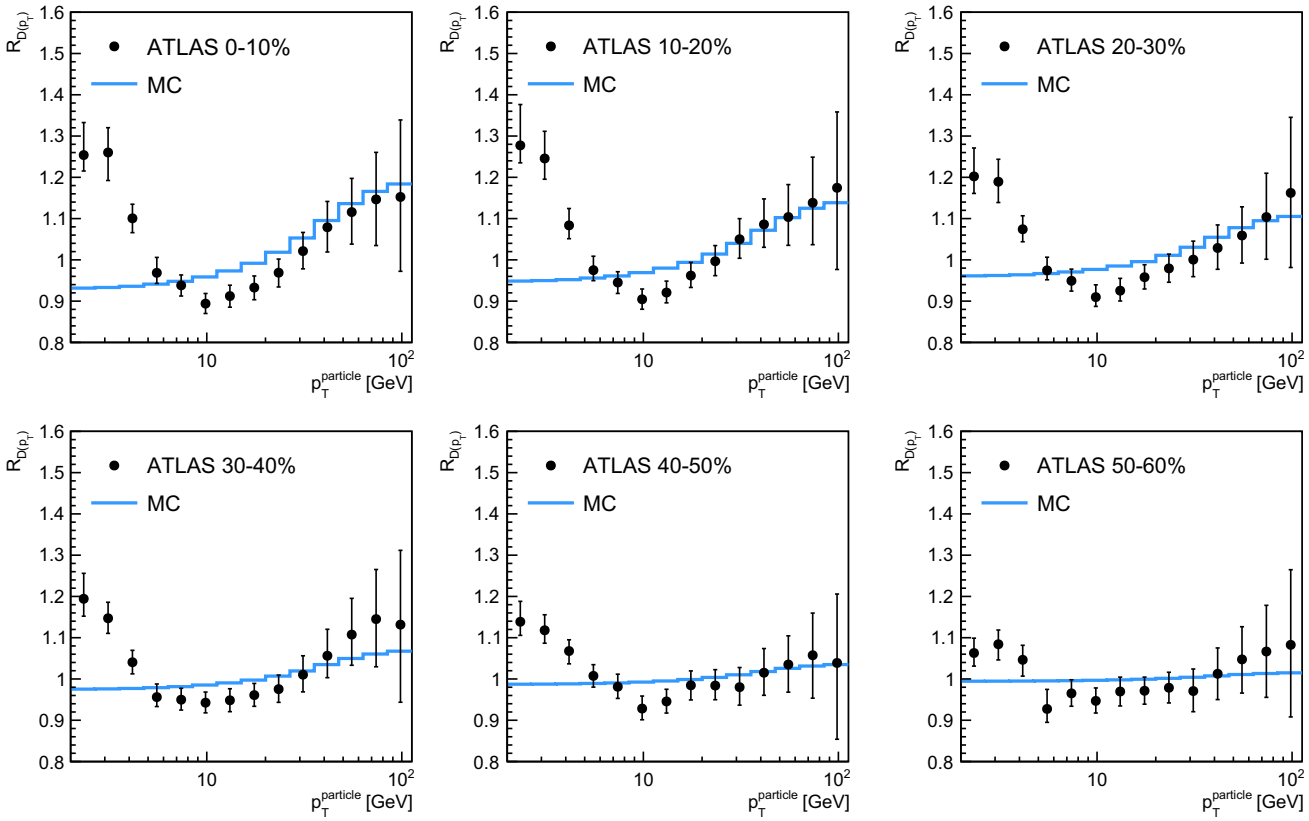

Fig. 12 Ratios of $D(p_{\mathrm{T}}^{\mathrm{ch}})$ distributions for six bins in collision centrality to those in peripheral (60–80 %) collisions, $D(p_{\mathrm{T}}^{\mathrm{ch}})|_{\mathrm{cent}}/D(p_{\mathrm{T}}^{\mathrm{ch}})|_{60-80}$, measured by ATLAS for $R = 0.4$ jets [12] (*black points*) are compared to the MC calculation (*blue histogram*) of the same quantity in the non-constant fractional energy loss model

produces changes in the fragmentation functions of lower-$p_{\mathrm{T}}^{\mathrm{jet}}$ jets different from that observed in the $p_{\mathrm{T}}^{\mathrm{jet}} > 100$ GeV jets cannot be excluded.

8 $D(z)$ low-z excess

As described above, our model for the modification of the fragmentation function in Pb+Pb collisions is based on the assumption that energy lost during the evolution of a parton shower in the medium does not appear as part of the measured jet and that the final fragmentation products have the same $D(z)$ distribution as if the reduced-energy jet fragmented in vacuum. While the validity of these assumptions may be debated (next section), the soft excess in the Pb+Pb $D(z)$ distributions, which cannot be explained by the different quark and gluon quenching, presents a manifest violation of the assumptions of the model. Supposing that the enhancement at low-z reflects either radiation within the jet, recoil partons, or collective response of the medium, from the point of view of our model, the extra low-z hadrons provide an upward shift of the jet energy. In the ATLAS Pb+Pb fragmentation function measurement, the excess fragments in the range $0.02 < z < 0.04$ were found to contribute ∼2 % of the jets transverse momentum for the 0–10 % centrality bin. Since that estimate could not account for contributions from hadrons below the minimum transverse momentum of the charged particle measurement, it is clearly an underestimate of the contribution of "excess" low-z partons to the jets energy. However, we take this number to be an order-of-magnitude estimate of the fractional contribution of the low-z excess to the energy of the typical jet which we will refer to as Φ^{soft}.

Since the energy in the low-z fragments likely is proportional to the jets energy, we assume that

$$\Phi^{\mathrm{soft}}_{\mathrm{inc}} = f_q^{\mathrm{int}}\Phi^{\mathrm{soft}}_q + (1 - f_q^{\mathrm{int}})\Phi^{\mathrm{soft}}_{\mathrm{g}}, \tag{20}$$

with $\Phi^{\mathrm{soft}}_{\mathrm{g}} = c_F\Phi^{\mathrm{soft}}_q$ and where Φ^{soft}_q, $\Phi^{\mathrm{soft}}_{\mathrm{g}}$, and $\Phi^{\mathrm{soft}}_{\mathrm{inc}}$ represent the average soft excess in quark, gluon, and all jets, respectively. The contribution of the excess soft hadrons to the jet energy is, in principle, already effectively accounted for in our analysis of the jet suppression where it will reduce S. However, it could affect our description of the modified fragmentation functions by increasing the jet energy that appears in the denominator of the z definition in the data by a fraction $1 + \Phi^{\mathrm{soft}}$, and, thus, reducing the z values by a factor $1/(1 + \Phi^{\mathrm{soft}})$. Thus, the modification of the frag-

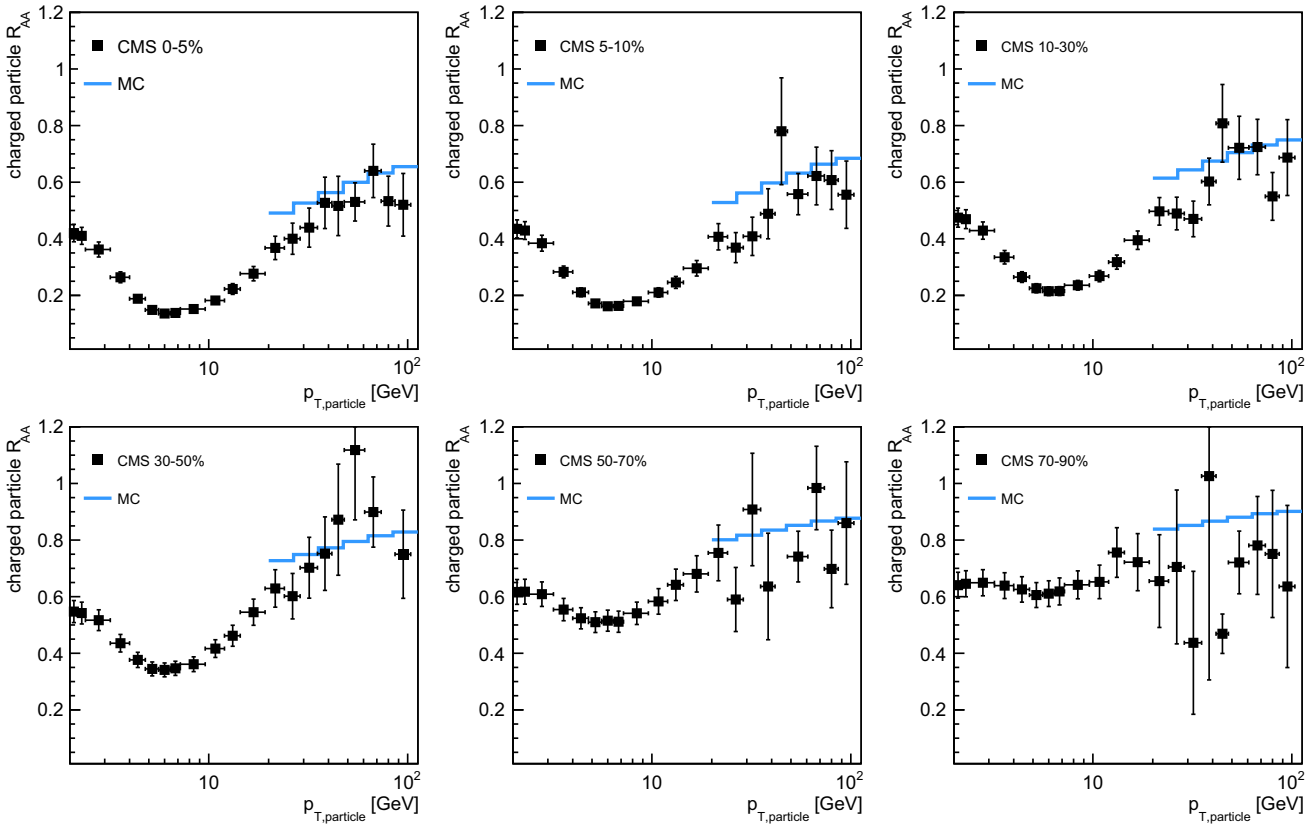

Fig. 13 Nuclear modification factor of charged particles measured by CMS [9] in six centrality bins (*black points*) is compared to the MC calculation of the same quantity in the non-constant fractional energy loss model (*blue histogram*)

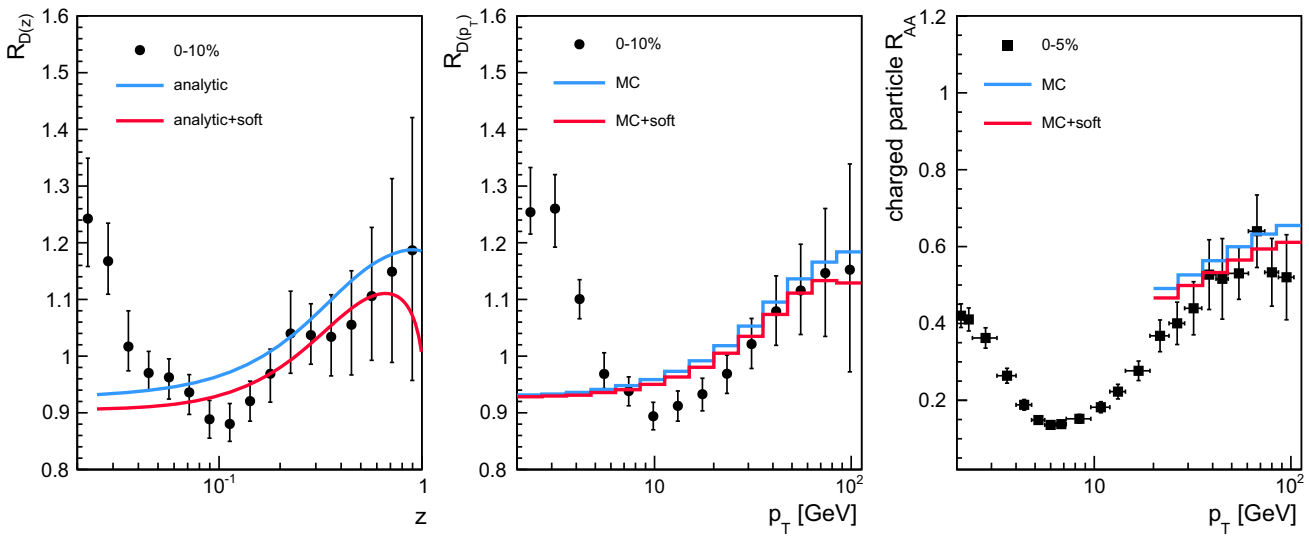

Fig. 14 Demonstration of the effects of accounting for the contribution of low-z particles in jet energies (see text). *Left* calculated $R_{D(z)}$ with (*red*) and without (*blue*) the low-z excess; *middle* same for $R_{D(p_T)}$; *right* R_{AA}^{ch} with and without the soft-z excess

mentation function in the data at z should correspond to the modification in our model at a z value of $z(1+\Phi_q^{soft})$. To reproduce that effect, we have corrected Eq. 14 follows,

$$D^{meas}(z) = f_q^{int} D_q(z[1+\Phi_q^{soft}]) + (1-f_q^{int}) D_g(z[1+\Phi_g^{soft}]), \quad (21)$$

and recalculated the $D(z)$ modifications taking $\Phi^{\rm soft}_{\rm inc} = 0.02$. The results are shown in the left panel of Fig. 14. Accounting for the shift in the jet energy shifts $R_{D(z)}$ down and leads to a better agreement between the data and the model. More than one sigma disagreement my now be seen only for the data point near $z = 0.1$.

The depletion seen in the modeled $R_{D(z)}$ at high-z reflects the rapid decrease in the parameterized $D(z)$ for $z \gtrsim 1$. The result in Fig. 14 is continuous across $z = 1$ for reasons given in Sect. 2, but the $D(z)$ still falls rapidly near $z = 1$. The data do not yet have the precision to resolve a change in behavior near $z = 1$ like that shown in the figure. Future measurements with improved precision could test for such an effect. Observing the depletion would provide strong empirical support to the picture that (most) jets fragment as in the vacuum but with additional energy from low-z particles whose origin is not yet understood.

The contribution of the excess soft hadrons to the jet momentum also influences the modeled $R_{D(p_{\rm T}^{\rm ch})}$ and $R^{\rm ch}_{\rm AA}$. The impact of this contribution can be avoided by reducing the quenched jet momentum used to look-up for the $D(p_{\rm T}^{\rm ch})$ distributions corresponding to quenched jets by $\Phi^{\rm soft}$. The impact of this on modeled $R_{D(p_{\rm T}^{\rm ch})}$ and $R^{\rm ch}_{\rm AA}$ for $\Phi^{\rm soft} = 0.02$ is shown in the middle and right panel of Fig. 14, respectively. While the impact of soft excess hadrons on the $D(p_{\rm T}^{\rm ch})$ distribution is rather small the impact on $R^{\rm ch}_{\rm AA}$ is more significant leading to a better agreement of modeled $R^{\rm ch}_{\rm AA}$ with the data.

9 Discussion

This paper has presented an analysis of implications of recent data on single jet suppression and inclusive jet fragmentation in Pb+Pb collisions. The analysis was based on a simple model for the quenching of a parton shower in the medium, namely that the parton shower loses energy to the medium in a manner such that the lost energy does not appear within the jet "cone". The fragmentation of the resulting jet was assumed to be the same as the fragmentation of a jet in vacuum. These assumptions may seem unreasonably simplistic given the current understanding of the evolution of high-energy parton showers in vacuum where perturbative calculations can describe many features of the resulting distributions of fragments. However, studies of the impact of the medium on the color-coherence of parton showers [17] suggest that the medium is unable to resolve the internal structure of many jets. According to Ref. [16] those jets interact with the medium as if they consist of a single color charge, and the reduced-energy jet fragments as if it were in vacuum. An extensive analysis of the angular and longitudinal momentum distribution of the radiated energy [16,31–34] indicates that the medium-induced radiation flow to large angles consistent with CMS measurements [15]. The combination of these two idea/results suggests a picture for jet-medium interactions that is qualitatively similar to that used in this analysis.

Important parameter of theoretical calculations involving the color-coherence effects is the medium resolution parameter, $R_{\rm med}$. In Ref. [17] authors show that there is a large probability for fragments not being resolved by the medium for the resolution parameter $R_{\rm med} = 0.2$. Further in the text authors argue that the resolution probability exhibits only a mild dependence on the jet radius. Also the experimental data [12,21] show that the jet $R_{\rm CP}$ and the jet fragmentation functions do not exhibit a substantial dependence on the jet radius. Therefore the assumptions described above should be applicable for $R = 0.4$ jets used in this study. It is clear that for the cases when more emitter structure is resolved by the medium, the color factor will be different from $9/4$ which we use here as a first approximation. The aim of future works in this direction should be to extract the value of the effective color factor directly from the data. For this, however, more differential measurements are needed.

This work started from a simple hypothesis that the $p_{\rm T}^{\rm jet}$ dependence of the measured jet $R_{\rm AA}$ and the modifications to the jet fragmentation functions could both be explained by the different quenching of quarks and gluons and the $p_{\rm T}^{\rm jet}$ dependence of the primordial quark fraction. Indeed, the first result using analytic expressions, power-law spectra and a constant fractional shift provided remarkably good agreement with both the $R_{\rm AA}$ and the $D(z)$ data. However, that success was short-lived as it was found to disagree with a Monte-Carlo implementation that used the PYTHIA8 quark and gluon spectra directly. When deviations of the spectrum from the pure power-law form were accounted for, the discrepancy between analytic and Monte-Carlo results was resolved, but the constant-fractional shift could no longer describe the data. The sensitivity of the jet $R_{\rm AA}$ to the shape of the jet spectrum is well known, but this analysis provides clear demonstration of the sensitivity of interpretations of the $R_{\rm AA}$ measurements to the accuracy in the description of the primordial jet spectra.

The analysis presented in this paper appears to rule out the possibility of a constant fractional shift parameterization of the effects of quenching on the jet spectrum. While a constant fractional shift is incompatible with most energy loss calculations, the weak $p_{\rm T}^{\rm jet}$ dependence of the measured jet suppression has often been (informally) interpreted as indicating fractional energy loss. However, as shown in Fig. 4, even when accounting for the fact that $f_{\rm q}$ increases with $p_{\rm T}^{\rm jet}$, a constant fractional energy loss produces an $R_{\rm AA}$ that decreases with $p_{\rm T}^{\rm jet}$ due to the fact the the primordial jet spectrum steepens relative to a pure power law with increasing $p_{\rm T}^{\rm jet}$. The $p_{\rm T}^{\rm jet}$-dependent shift extracted from the data, in fact, varies like $\sqrt{p_{\rm T}^{\rm jet}}$ as predicted in Ref. [27]. That reference makes clear that the shift should not necessarily be interpreted as the average energy loss of the jets. Indeed, the shift

approximately parameterizes the convolution of the energy loss distribution with the primordial jet spectrum. Clearly lacking in the model is the implementation of fluctuations of the jet quenching and its path-length dependence. Thus parameters used in the model should be viewed as effective parameters. The direct interpretation of values of α or s' is not immediately possible. Nonetheless, it is remarkable that with the simple centrality dependence of s' observed in Fig. 7, the full $p_{\mathrm{T}}^{\mathrm{jet}}$ and centrality dependence of the jet suppression can be accounted for by three parameters, α and the effective slope and intercept of the N_{part} dependence of s'.

The apparent accidental cancellation of the variation of spectrum shapes and quark fraction observed here and in Ref. [35] that leads to the measured constancy of R_{AA} with rapidity [11] is unfortunate as it reduces the sensitivity of the measurement to features of the energy loss that could help to test or constrain calculations of medium-induced energy loss. However, the extensions of our analysis to larger rapidity indicate that at larger rapidities, the increased curvature of the primordial jet spectra will provide a different and stronger variation of R_{AA} with $p_{\mathrm{T}}^{\mathrm{jet}}$. That is particularly true in the $2.8 < |y| < 3.5$ bin where measurements may be difficult in the most central collisions but could be performed in more peripheral centrality bins where the effect should still be measurable.

The analysis in this paper suggests that much or all of the observed modifications to the jet fragmentation functions in Pb+Pb collisions can arise from the different quenching of quark and gluon jets – *except for the enhancement at low* z. This observation could have important implications for the theoretical understanding of the quenching physics. For example, in the context of the picture presented in Ref. [17] where quenching of the jets is influenced by the ability of the medium to resolve the internal structure of the jet, jets that are not resolved by the medium fragment according to their vacuum fragmentation functions. But, the measured $D(z)$ distributions will still differ from those in pp or peripheral Pb+Pb collisions due to the different energy loss of the quarks and gluons. On the other hand, if the fragmentation functions of the quark and gluon jets are separately modified, then we would have to conclude that the medium is resolving the internal structure of the jet. The simplicity of the analysis used in this paper is not adequate to draw a firm conclusion that the $D(z)$ modifications at intermediate and large z can be completely attributed to flavor-dependent quenching. While MC generators which model the jet quenching implement the difference in the treatment of quark and gluon jets, this analysis shows that the effects of different quark and gluon quenching should be addressed explicitly in future analyses of the fragmentation functions. Measurements of jet fragmentation in γ-jet events, where the jet spectrum has a larger quark fraction would be valuable in addressing this issue.

The analysis in this paper suggests that the magnitude and transverse momentum dependence of charged particle R_{AA} for particles with $p_{\mathrm{T}} > 20$ GeV can largely result from the different quenching of quark and gluon jets as well. The disagreement between the measured charged particle R_{AA} and the R_{AA} in the model, namely larger suppression and steeper R_{AA} as a function of p_{T} seen in the data, remains to be understood. It may be arising from missing physics in the model, difference between the measured charged particle spectra and their PYTHIA8 simulation, or from larger contribution of soft particles to quenched jets at lower p_{T}. Irrespective of the source of this disagreement, the result clearly points to the importance of understanding the measurements involving single particles in the context of fully reconstructed jets.

As described above, the enhanced production of hadrons at low z observed in data [12,13] cannot be explained by the different energy loss of quarks and gluons. It's also interesting that it could not be explained by a strong-coupling calculation of energy loss [36] but did arise in a collisional energy-loss scenario also tested in that same paper, suggesting that the excess could arise from recoiling constituents of the medium [37]. If this explanation is correct, then the low-z excess is directly probing (part of) the medium-response to the passage of jets. An alternative explanation was provided in Ref. [34] that showed a soft-z excess can arise when the medium resolves the constituents of the jet core. More speculatively, it might be that the excess arises from the collective response of the medium such as a diffusion wake [38]. Regardless of the explanation, the energy contributed to the low-z particles acts in the context of our model as an extra contribution of the energy of the jet. The effect of this contribution produces modest but noticeable effects on the fragmentation functions. We note that the persistence of the low-z excess in non-central collisions indicates that it does not result from systematics in the measurement. Given the potential importance of the low-z excess, more detailed measurements in non-central events where the effects of the underlying event are smaller may be warranted.

10 Conclusions

This paper has presented an analysis of single jet measurements from Pb+Pb collisions at the LHC using a simple, phenomenological model. The analysis used quark and gluon spectra obtained from PYTHIA8 and applied the "shift" formulation described by Baier et al. to describe the single-jet suppression. The modifications to the jet fragmentation functions were assumed to result from the different quenching of quarks and gluons assuming that the quenched jets fragment as they do in vacuum.

Our analysis showed that the transverse momentum dependence of the quark fraction plays a role in the evolution

of the jet R_{AA} with $p_{\mathrm{T}}^{\mathrm{jet}}$ as was also observed in Ref. [35]. However, the curvature of the primordial jet spectrum relative to a pure power-law also substantially effects the R_{AA}. The data were found to be incompatible with a constant fractional shift, $S = sp_{\mathrm{T}}^{\mathrm{jet}}$. Fits of the data using a shift that varied with $p_{\mathrm{T}}^{\mathrm{jet}}$ as $\left(p_{\mathrm{T}}^{\mathrm{jet}}\right)^{\alpha}$ yielded a value $\alpha \sim 0.55$ compatible with the prediction in Ref. [27]. The measured modifications of the inclusive jet fragmentation functions can be largely explained as resulting from the different quenching of quarks and gluons. More specifically, the suppression of the fragmentation function at intermediate z and the enhancement in the fragmentation function at large z reflect the different shapes of the quark and gluon fragmentation functions and the increase in the quark fraction due to the greater energy loss of gluon jets. However, our model is not able to account for the low-z enhancement in the Pb+Pb fragmentation functions. If our analysis is correct, the fragmentation function modifications provide a direct test of the color-charge dependence of jet quenching. The model can explain most of the observed suppression of the charged particle yield at high $p_{\mathrm{T}}^{\mathrm{ch}}$ though it slightly under-predicts the amount of suppression and has a weaker $p_{\mathrm{T}}^{\mathrm{ch}}$ dependence at the lowest $p_{\mathrm{T}}^{\mathrm{ch}}$ values included in the analysis.

Because the quark fraction varies as a function of rapidity, both the R_{AA} and the $D(z)$ modifications should evolve as a function of rapidity, though the rapidity-dependent evolution of the quark and gluon spectra appears to cancel out the effects of the changing quark fraction over the rapidity range measured in the ATLAS data. Predictions are made for R_{AA} and $R_{D(z)}$ at large rapidity that would allow the conclusions of this analysis to be tested.

Acknowledgments The work of MS was supported by Charles University in Prague, Projects PRVOUK P45 and UNCE 204020/2012. BAC's research was supported by the US Department of Energy Office of Science, Office of Nuclear Physics under Award No. DE-FG02-86ER40281. We would like to thank Aaron Angerami for many useful discussions regarding the issues raised in this paper.

Funded by SCOAP[3].

Appendix

In this appendix section we provide the full equation for the R_{AA} in the case of extended power-law parameterization of the jet spectra discussed in Sect. 4. The equation reads as follows

$$
\begin{aligned}
R_{\mathrm{AA}} = {} & f_q \left(\frac{1}{1+S_q/p_{\mathrm{T}}^{\mathrm{jet}}}\right)^{n_q+\beta_q \log((p_{\mathrm{T}}^{\mathrm{jet}}+S_q)/p_{\mathrm{T}0})} \\
& \times \left(\frac{p_{\mathrm{T}0}}{p_{\mathrm{T}}^{\mathrm{jet}}}\right)^{\beta_q \log(1+S_q/p_{\mathrm{T}}^{\mathrm{jet}})} \left(1+\frac{dS_q}{dp_{\mathrm{T}}^{\mathrm{jet}}}\right) \\
& + (1-f_q) \left(\frac{1}{1+S_g/p_{\mathrm{T}}^{\mathrm{jet}}}\right)^{n_g\beta_g \log((p_{\mathrm{T}}^{\mathrm{jet}}+S_g)/p_{\mathrm{T}0})} \\
& \times \left(\frac{p_{\mathrm{T}0}}{p_{\mathrm{T}}^{\mathrm{jet}}}\right)^{\beta_g \log(1+S_g/p_{\mathrm{T}}^{\mathrm{jet}})} \left(1+\frac{dS_g}{dp_{\mathrm{T}}^{\mathrm{jet}}}\right), \qquad (22)
\end{aligned}
$$

where the $p_{\mathrm{T}}^{\mathrm{jet}}$ dependent flavor fraction is calculated as

$$
f_q\left(p_{\mathrm{T}}^{\mathrm{jet}}\right) = \frac{1}{1+\left(\frac{1-f_{q0}}{f_{q0}}\right)\left(\frac{p_{\mathrm{T}0}}{p_{\mathrm{T}}^{\mathrm{jet}}}\right)^{n_g-n_q+(\beta_g-\beta_q)\log\left(p_{\mathrm{T}}^{\mathrm{jet}}/p_{\mathrm{T}0}\right)}}. \qquad (23)
$$

References

1. N. Armesto, B. Cole, C. Gale, W.A. Horowitz, P. Jacobs et al., Phys. Rev. C **86**, 064904 (2012)
2. Y. Mehtar-Tani, J.G. Milhano, K. Tywoniuk, Int. J. Mod. Phys. A **28**, 1340013 (2013)
3. ATLAS Collaboration, Phys. Rev. Lett. **105**, 252303 (2010)
4. J. Adams et al., Phys. Rev. Lett. **91**, 172302 (2003)
5. A. Adare et al., Phys. Rev. Lett. **101**, 232301 (2008)
6. S.S. Adler et al., Phys. Rev. C **69**, 034910 (2004)
7. ALICE Collaboration, Phys. Lett., B **720**, 52–62 (2013)
8. ATLAS Collaboration, ATLAS Note (2012). ATLAS-CONF-2012-120
9. CMS Collaboration, Eur. Phys. J. C **72**, 1945 (2012)
10. K.M. Burke et al., Phys. Rev. C **90**(1), 014909 (2014)
11. ATLAS Collaboration, Phys. Rev. Lett. **114**(7), 072302 (2015)
12. ATLAS Collaboration, Phys. Lett. B **739**, 320–342 (2014)
13. CMS Collaboration, Phys. Rev. C **90**, 024908 (2014)
14. T. Sjstrand, S. Ask, J.R. Christiansen, R. Corke, N. Desai et al., Comput. Phys. Commun. **191**, 159–177 (2015)
15. CMS Collaboration, Phys. Rev. C **84**, 024906 (2011)
16. J.-P. Blaizot, E. Iancu, Y. Mehtar-Tani, Phys. Rev. Lett. **111**, 052001 (2013)
17. J. Casalderrey-Solana, Y. Mehtar-Tani, C.A. Salgado, K. Tywoniuk, Phys. Lett. B **725**, 357–360 (2013)
18. J. Casalderrey-Solana, D.C. Gulhan, J.G. Milhano, D. Pablos, K. Rajagopal, JHEP **1410**, 19 (2014)
19. M. Gyulassy, P. Levai, I. Vitev, Jet quenching in thin quark gluon plasmas. 1. Formalism. Nucl. Phys. B **571**, 197–233 (2000)
20. I. Vitev, Phys. Lett. B **606**, 303–312 (2005)
21. ATLAS Collaboration, Phys. Lett. B **719**, 220–241 (2013)
22. ATLAS Collaboration, Eur. Phys. J. C **74**(8), 2965 (2014)
23. ATLAS Collaboration, ATLAS Note (2012). ATL-PHYS-PUB-2012-003
24. H.-L. Lai, M. Guzzi, J. Huston, Z. Li, P.M. Nadolsky et al., Phys. Rev. D **82**, 074024 (2010)
25. M. Cacciari, G.P. Salam, G. Soyez, JHEP **04**, 063 (2008)

26. D. de Florian, R. Sassot, M. Stratmann, Phys. Rev. D **75**, 114010 (2007)
27. R. Baier, Y.L. Dokshitzer, A.H. Mueller, D. Schiff, JHEP **0109**, 033 (2001)
28. K. Adcox et al., Nucl. Phys. A **757**, 184–283 (2005)
29. ATLAS Collaboration, JHEP **1502**, 153 (2015)
30. S. Chatrchyan et al., JHEP **1206**, 036 (2012)
31. J.-P. Blaizot, F. Dominguez, E. Iancu, Y. Mehtar-Tani, JHEP **1301**, 143 (2013)
32. J.-P. Blaizot, F. Dominguez, E. Iancu, Y. Mehtar-Tani, JHEP **1406**, 075 (2014)
33. J.-P. Blaizot, L. Fister, Y. Mehtar-Tani, Nucl. Phys. A **940**, 67–88 (2015)
34. J.-P. Blaizot, Y. Mehtar-Tani (2015)
35. T. Renk, arXiv:1406.6784 (unpublished)
36. J. Casalderrey-Solana, D.C. Gulhan, J.G. Milhano, D. Pablos, K. Rajagopal, Nucl. Phys. A **931**, 487–492 (2014)
37. K. Zapp, J. Stachel, U.A. Wiedemann, PoS, High-pT physics **09**, 022 (2009)
38. S.S. Gubser, S.S. Pufu, A. Yarom, Phys. Rev. Lett. **100**, 012301 (2008)